Materials Today Bio 16 (2022) 100388

Contents lists available at ScienceDirect

Materials Today Bio

journal homepage: www.journals.elsevier.com/materials-today-bio

The application of 3D bioprinting in urological diseases

Kailei Xu [a,b,c,d,e,1], Ying Han [d,e,1], Yuye Huang [a,b], Peng Wei [a], Jun Yin [d,e,**], Junhui Jiang [f,g,*]

[a] Department of Plastic and Reconstructive Surgery, Ningbo First Hospital, Ningbo 315010, China
[b] Center for Medical and Engineering Innovation, Central Laboratory, Ningbo First Hospital, Ningbo 315010, China
[c] Key Laboratory of Precision Medicine for Atherosclerotic Diseases of Zhejiang Province, Ningbo 315010, China
[d] The State Key Laboratory of Fluid Power and Mechatronic Systems, School of Mechanical Engineering, Zhejiang University, Hangzhou 310028, China
[e] Key Laboratory of 3D Printing Process and Equipment of Zhejiang Province, School of Mechanical Engineering, Zhejiang University, Hangzhou 310028, China
[f] Translational Research Laboratory for Urology, The Key Laboratory of Ningbo, Ningbo First Hospital, Ningbo, 315010, China
[g] Department of Urology, Ningbo First Hospital, Ningbo, 315010, China

ARTICLE INFO

Keywords:
Tissue engineering
Tumor microenvironment
Kidney regeneration
Urethral replacement
Urological cancer

ABSTRACT

Urologic diseases are commonly diagnosed health problems affecting people around the world. More than 26 million people suffer from urologic diseases and the annual expenditure was more than 11 billion US dollars. The urologic cancers, like bladder cancer, prostate cancer and kidney cancer are always the leading causes of death worldwide, which account for approximately 22% and 10% of the new cancer cases and death, respectively. Organ transplantation is one of the major clinical treatments for urological diseases like end-stage renal disease and urethral stricture, albeit strongly limited by the availability of matching donor organs. Tissue engineering has been recognized as a highly promising strategy to solve the problems of organ donor shortage by the fabrication of artificial organs/tissue. This includes the prospective technology of three-dimensional (3D) bioprinting, which has been adapted to various cell types and biomaterials to replicate the heterogeneity of urological organs for the investigation of organ transplantation and disease progression. This review discusses various types of 3D bioprinting methodologies and commonly used biomaterials for urological diseases. The literature shows that advances in this field toward the development of functional urological organs or disease models have progressively increased. Although numerous challenges still need to be tackled, like the technical difficulties of replicating the heterogeneity of urologic organs and the limited biomaterial choices to recapitulate the complicated extracellular matrix components, it has been proved by numerous studies that 3D bioprinting has the potential to fabricate functional urological organs for clinical transplantation and *in vitro* disease models.

1. Urological diseases and the application of tissue engineering

The urinary system, also known as the renal system, consists of kidneys, ureters, the bladder, and the urethra. It acts not only as the drainage system eliminating waste from the body, but also regulates blood volume and pressure, controls the level of electrolytes, and regulates blood pH. Urological disorders and diseases are common global health problems, leading to significant healthcare expenditures, substantial disabilities, impaired life quality and shortened survival times for patients [1]. The urological diseases and disorders being covered by this review mainly include chronic kidney disease, urethral stricture, kidney cancer, bladder cancer, and prostate cancer (PCa). Chronic kidney disease and urethral stricture require organ/tissue transplantation for better treatment, which was limited by the availability of matching donor organs and a high risk of organ rejection. Kidney cancer, bladder cancer, and prostate cancer are the leading causes of death worldwide due to the limitation of drug development.

The kidney (renal) plays a central role in the urinary system in metabolism and drug elimination. Chronic kidney disease results in the long-term loss of kidney function, affecting more than 700 million people around the world [2]. Among them, 20% of patients with the progressive loss of kidney function suffer from end-stage renal disease (ESRD) [3]. ESRD patients have to be placed on life-saving renal replacement therapies such as haemodialysis and peritoneal dialysis while waiting for

* Corresponding author. Translational Research Laboratory for Urology, The Key Laboratory of Ningbo, Ningbo First Hospital, Ningbo, 315010, China.
** Corresponding author. Key Laboratory of 3D Printing Process and Equipment of Zhejiang Province, School of Mechanical Engineering, Zhejiang University, Hangzhou, 310028, China.
E-mail addresses: junyin@zju.edu.cn (J. Yin), jiangjh200509@126.com (J. Jiang).
[1] These authors contributed equally to this work.

https://doi.org/10.1016/j.mtbio.2022.100388
Received 13 June 2022; Received in revised form 24 July 2022; Accepted 27 July 2022
Available online 2 August 2022

kidney transplantation [4] that is limited by the availability of matching donor organs and a high risk of organ rejection [5]. Other kidney diseases include kidney (renal) cancer, kidney stone, glomerulonephritis, and pyelonephritis. Among these, renal cancer is one of the most critical malignancies, with more than 131,000 deaths and 342,000 incident cases occurring each year globally. Approximately 90% of renal cancers are renal cell carcinoma (RCC) [6,7], which is derived from the proximal tubular epithelial cells of the renal cortex. About one-third of RCC patients will further present metastatic disease that causes the most of lethal cases for it is almost incurable [8,9].

The bladder is a hollow organ in the lower part of the urinary system. Bladder diseases, such as bladder calculus, inflammation and bladder cancer, could lead to frequent urination, urgency, dysuria and hematuria, that strongly affect patients' life quality. Cancer is one of the most critical diseases of the bladder with its incidence rate increasing with age; people aged 50–70 have the highest incidence rates, and this rate for men is 3–4 times that of women when caused by smoking tobacco [10–12]. Most bladder cancers are diagnosed at an early stage when the condition is highly curable. However, even at this stage, bladder cancers can recur after successful treatment and still develop to metastasis.

The prostate locates in the lesser pelvis and belongs to the male reproductive system. Prostate diseases, such as inflammation, benign prostatic hyperplasia and cancer, can damage the function of urinary system as the prostate acts as a muscle-driven mechanical switch for urination. PCa is a commonly diagnosed cancer type and the leading cause of death for men worldwide. Around 33% of males in The United States will be diagnosed with PCa and 1 out 33 will die from it [13]. Primary PCa is curable, while metastatic PCa has poor prognosis and causes most of the fatal cases. Instead of soft tissues like the lung and lymph nodes, PCa preferentially metastasizes to bone and demonstrates osteoblastic or osteolytic phenotypes, causing the formation of woven bone and leading to more severe symptoms [14]. Androgen-deprivation therapy is commonly used to treat metastatic PCa, while it frequently develops to androgen-independent and castration-resistant PCa (CRPC) [15,16], which is an advanced form of PCa with few treatment options and low survival rates [17].

The urethra is part of the body's drainage system for removing urine, which passes through the bladder and the prostate. Urethral stricture is one of the most frequently diagnosed diseases of the urethra, which scars the submucosal tissue of the corpus spongiosum, leading to urethral lumen constriction. The common causes of urethral stricture include surgery that involves inserting an instrument, trauma or injury to the urethra or pelvis, and urethral or PCa. Approximately 0.6% of males are diagnosed for urethral stricture due to a variety of etiological factors [18]. The surgical repair of urethral stricture has always been one of the most challenging subjects studied by urologists.

Organ transplantation is among the most effective treatments for severe urological diseases, like ESRD and urethral stricture. For urologic cancers, although chemotherapy and radiotherapy are frequently used, full organ resection could be also performed for higher survival rate. Radical prostatectomy is one of the most common treatments for localized PCa. Around 30% of the patients with localized PCa would be performed with prostatectomy [19], which was more than 100,000 patients annually [20]. Radical nephrectomy is the gold standard treatment for localized RCC [21], while it also causes significant decreases in renal function and chronic renal insufficiency, which significantly increase the risk of cardiovascular events and overall mortality [22]. Similar post-surgery issues were also observed for radical cystectomy [23], which is the complete bladder removal for bladder cancers. Therefore, the transplantation was also required for these organs after cancer removal to improve the patient recovery and life quality.

However, due to the limited global availability of matching donor organs and the immunological responses to animal organs, artificial organs could be a potential choice in the future for clinical transplantation. Tissue engineering is a multidisciplinary field combing life science and engineering principles to investigate and develop biological substitutes to repair and restore tissue functions [24], which could be a promising direction to solve the problem of organ donor shortage for urological diseases (Fig. 1). To generate functional biological substitutes, biomaterial scaffolds and cells are the two main components [25]. Ideally, the best approach is to isolate primary stem cells or progenitor cells from patients, scale them up *in vitro*, culture them on scaffolds, differentiate them into the desired lineage phenotypes through the induction of conditional media, and implant cell-seeded scaffolds into injured sites in patients. This could be a potential solution to greatly reduce the immunological response to the implants and develop personalized treatments.

Tissue engineering has been widely investigated for urological diseases due to the shortage of donor organ availability. Decellularized extracellular matrix (dECM) scaffolds transplanted for renal regeneration in a nephrectomized rat model have shown increased renal size and the regeneration of renal parenchyma cells in the repair area containing the grafted scaffold [26,27]. Bioengineered bladder tissues developed with collagen-based scaffolds containing autologous cells have shown potential application for patients who need cystoplasty [28,29]. Scaffolds made with silk/keratin enhanced the tissue repair in a dog urethral defect model and yielded organized muscle bundles and epithelial layer, which demonstrated their potential application for urethral disease [30,31].

Apart from biomaterial composition and cell type, the architecture and topology of tissue engineering scaffolds also play a critical role in tissue regeneration. Higher porosity and larger pore size of cartilage scaffolds could promote ECM formation, nutrient diffusion and host cell infiltration, which supported successful osteochondral regeneration *in vivo*. [32] Well-defined nanoarrays of RGD (Arg-Gly-Asp) peptides on poly (ethylene glycol) (PEG) hydrogels were able to regulate the spreading area and differentiation of rat mesenchymal stem cells (MSCs) [33], influencing the functionality of regenerated tissues. A rougher biomaterial surface was found to significantly promote MSCs biomineralization and osteogenic marker expression on poly(ε-caprolactone) (PCL) [34]. However, such personalized architectures and topology requirements were difficult to achieve by traditional fabrication processes, like mold casting and electrospinning.

2. Commonly used 3D bioprinting technologies in urological diseases

3D printing is one of the latest technologies used in many industries, such as education, food, fashion, transportation, and health. Bioprinting is one of the 3D printing types that refers to the application in the life science industry, and is commonly used in tissue engineering for the development of scaffolds with complicated architectures that mimic native organs and can be eventually used for clinical transplantation [35–38]. Compared with traditional tissue engineering methods, 3D bioprinting could provide: 1) High printing resolution. The porosity, pore size, nanoarrays, and roughness of tissue engineering scaffolds would strongly affect the nutrient diffusion, host cell infiltration, and the successfulness of tissue regeneration. 3D bioprinting could create more precise architectures and topology to better facilitate tissue regeneration, which were difficult to achieve by traditional fabrication processes, like mold casting and electrospinning. 2) Structure complexity and material heterogeneity. Urologic tissues, like kidney, prostate, and bladder, have completely different organ structures and ECM compositions, which is difficult to be reproduced by traditional tissue engineering methods. 3D bioprinting could better mimic the complexity and ECM distribution of urologic organs to facilitate tissue regeneration. 3) Personalization. Patients with urological diseases are commonly phenotypically different from each other, especially in urologic cancers, which causing the importance for the preparation of personalized tumor microenvironment (TME) for more accurate *in vitro* drug screening. 3D bioprinting could easily produce personalized organs or *in vitro* cancer models for clinical application compared with traditional tissue engineering methods.

3D bioprinting could be mainly classified into two subtypes, namely printing with cells (cell-laden) and without cells (cell-free). Cell-laden

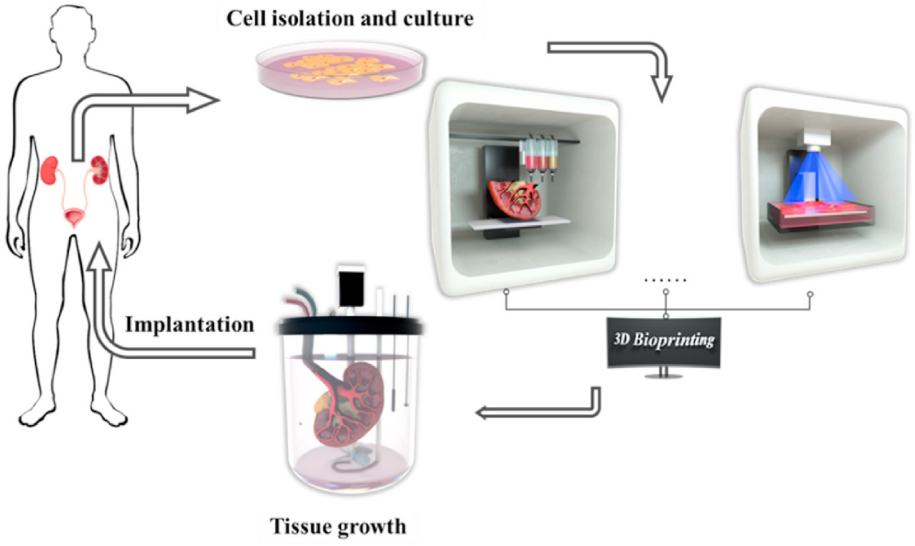

Fig. 1. Tissue engineering and three-dimensional (3D) bioprinting technologies for urological diseases.

bioprinting can deliver different types of cells to precise locations and form living constructs that better mimic the native organ structure and cell distribution. 3D bioprinted hyaluronic acid-based cell-laden scaffold was used to simulate the mechanical and biological properties of human brain microenvironment, which could be further used for glioblastoma multiforme invasion mechanism study and drug screening [39]. Liu et al. used multi-nozzle additive-lathe 3D bioprinting technology to produce a bilayer nerve conduit with bone marrow mesenchymal stem cells (BMSCs) in the inner layer and PC-12 cells at outer layer, which had great potential in facilitating peripheral nerve repair [40]. Cell-free bioprinting allows for more flexible material selection, complicated structures and higher mechanical strength, since cells can be seeded after printing and the cellular survival rate during the printing process can be neglected. Hydroxyapatite/tricalcium phosphate scaffold with hierarchical porous structure was seeded with NIH3T3 cells after 3D printing for bone regeneration [41]. Wang et al. combined 3D printing with freeze-casting to produce scaffolds with microscale pores in the struts and successfully supported the breast cancer cell growth [42]."

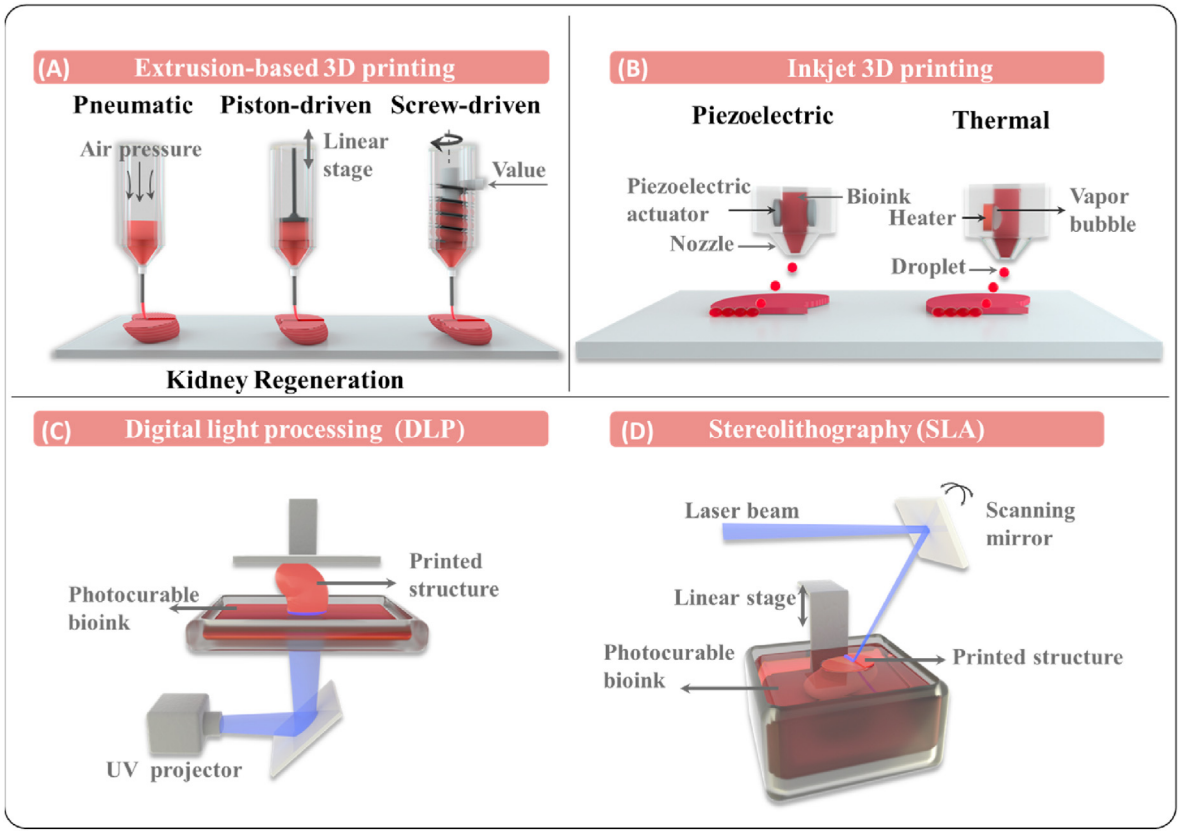

Fig. 2. 3D bioprinting technologies and comparisons. (a) Extrsusion-based bioprinting; (b) Inkjet-based bioprinting; (c, d) Light-assisted bioprinting.

2.1. Extrusion-based bioprinting

Extrusion-based bioprinting is one of the most broadly used biofabrication techniques (Fig. 2A), which was composed of a dispensing head (syringe, nozzle, and pressure system) and an automated three-axis robotic system. In the extrusion-based bioprinting process, bioink is deposited on a platform by sheer force through a nozzle in a controlled manner, which can move along three axes [43], resulting in customized 3D structures with precise cylindrical filaments. The printed structures can be further stabilized through ionic, photo-, and thermal crosslinking mechanisms that enable the application of almost any type of bioink with a wide range of viscosities, cell seeding density, printing speed and scalability for extrusion-based bioprinting [35]. Given the complicated structure and chemical properties of native organs and tissues, extrusion-based bioprinting can be set up with multiple dispensing heads and loaded with different types of bioinks containing various cells and materials, in order to better mimic the architecture and cellular distribution of tissues [44]. Utilizing the advantages of extrusion-based bioprinting, neurol stem cells (NSCs) can be loaded into a hydrogel mixture (chitosan, hyaluronic acid and Matrigel) and printed as NSCs-laden scaffolds for spinal cord injury repair [45]. Extrusion-based bioprinting has also been used to fabricate artificial kidneys [46], cartilages [47,48], osseous tissue [49], liver [50], etc.

2.2. Inkjet-based bioprinting

Inkjet-based bioprinting is a popular technology for depositing biological components, since it enables the delivery of thousands of material droplets in the picoliter volume range in a few seconds through a noncontact manner (Fig. 2B). Inkjet-based bioprinting can be mainly classified into two categories: continuous inkjet printing and drop-on-demand (DOD) inkjet printing. Continuous inkjet printing refers to the extrusion of bioink through an electric field that splits the column into droplets due to the Rayleigh−Plateau instability [51,52]. However, due to the ease of contamination, device complexity and difficulty of usage, this method is rarely used for bioprinting.

Compared with continuous inkjet printing, DOD inkjet printing has gained wider popularity since it releases droplets only when triggered. This approach mainly includes thermo, piezoelectric and electrostatic methods. Thermo DOD creates heat bubbles in the chamber, which squeeze bioink and produce droplets at the nozzle. The heating temperature rise to 250–350 °C in an extremely short period, while the overall bioink temperature only elevates by around 5 °C [53,54]. Thermo DOD is able to create droplets with a diameter of 30–80 μm, and has the benefits of low cost, ease of operation and maintenance. Piezoelectric inkjet printing generates tiny droplets through the deformation of extrusion chamber wall made with piezoelectric ceramics, which could cause a sudden volume change and lead to the ejection of droplets [55]. Droplets could be in the diameter range of 50–100 μm, which is adjustable by the modification of driving mode for piezoelectric elements and the voltage pulse characteristics. Piezoelectric inkjet printing has several unique advantages and thus been used to create single cell printing for tumor heterogeneity research [56]. In the electrostatic inkjet printing technique, the bioink is squeezed through the deformation of electrostatic plate, creating droplets with a diameter of 10–60 μm, which is much smaller compared with those in thermo and piezoelectric DOD [57].

Due to the advantages of inkjet droplets in picoliter-range printing and its high-throughput characteristics, vasculature inkjet printing has been widely investigated. Xu et al. used inkjet printing to create zigzag and bifurcated tubular structures with alginate-based bioink and NIH 3T3 mouse fibroblasts [58]. Searsona et al. employed piezoelectric DOD to fabricate microvessels with fibrinogen, in which embedded human umbilical venous cord endothelial cells (HUVECs) formed a confluent monolayer within 14 days, demonstrating itcats promising appliion in vasculature tissue engineering [59]. Overall, inkjet-based bioprinting has shown its promising potentials for the microstructure development in tissue engineering for scaffold building and cellular distribution.

2.3. Light-assisted bioprinting

Light-assisted bioprinting is a nozzle-free process, where 3D constructs are produced in a pattern defined by a pulsed light path (Fig. 2C and D). This technique is relatively gentle on cellular viability compared with extrusion-based and inkjet-based bioprinting [60]. The cellular viability for light-assisted bioprinting could reach 85%–95%, due to the absence of high temperatures or exertion of shear stress [61–63], while the cellular viability for extrusion-based bioprinting various from 40% to 90% based on the various nozzle size, printing temperature, and operation pressure [64–67]. The cellular viability for inkjet-based bioprinting could various from 70% to 90% depends on the inkjet types and nozzle size [57,68–70]. Laser-based and digital light processing (DLP) are the major light-assisted bioprinting methods. For laser-based bioprinting, the laser beam is focused on a donor slide containing bioink that is deposited on a collection plate as droplets. This type of bioprinting is capable of dispensing viscous and/or small volumes of bioink into a precise and fine pattern, while the process is relatively slow [71]. Compared with laser-based bioprinting, the time requirement of DLP is significantly shorter owing to a computer-controlled laser that projects a two-dimensional (2D) pattern on the bioink and produces an entire layer at once [72,73]. DLP has shown potential applications in the fabrication of engineered bone grafts [74,75], in a liver cancer model [76], and multivascular networks [77].

2.4. Commonly used bioinks

The commonly used bioinks are composed of natural or synthetic biomaterials (See Table 1) [78]. Most of the natural biomaterials can be bioprinted while cell-laden due to the weak mechanical properties and relatively gentle printing process [79]. Meanwhile, for synthetic biomaterials, the printing process is often accompanied by high shear stress and temperature, and cells commonly have to be seeded after printing [80].

Collagen is one of the major ECM components in urological organs and is also correlated with urological disease progression. In kidney, the interstitial matrix of the kidney is also mainly comprised with collagen type I and III [81], and the up-regulation of collagen was found to be correlated with renal fibrosis and has been recognized as the biomarker to delineate the pathological alterations to the ECM during chronic kidney disease progression [81–84]. Human embryonic kidney cells in agarose-collagen bioink were reported to proliferate within the printed structures, and could be potentially used for kidney regeneration [85]. Highly controlled and reproducible renal TME created with collagen-based bioink has shown potential applications for anticancer drug screening [86]. In prostate, collagen comprises more than 12% among the 120 types of ECM proteins [87,88], and the deregulation of collagen metabolism was also correlated with PCa Gleason score and could be a predictor of patient survival [89–92]. In bladder, collagen is commonly found in the connective tissue outside the muscle bundles of bladder wall [93,94] and the ratio of type III to type I collagen has been observed to be abnormally elevated in patients with bladder disease compared with normal bladder [95–97]. Although collagen has not been used in 3D bioprinting for prostate and bladder diseases, it should be an ideal bioink for these applications in the future development.

Gelatin is a natural form of hydrolyzed collagen, which retains collagen's high biocompatibility and cellular adhesion properties. Native gelatin can also form hydrogel only by thermo-crosslinking like collagen, leading to the methylation modification to develop gelatin-methacryloyl (GelMA) for wider use in cell-laden bioprinting. The cellular viability of GelMA in bioprinting has been verified using numerous cell types, such as liver cells [98], nerves cells [99] and BMSCs [100,101]. Gelatin and GelMA have been 3D bioprinted for *in vitro* kidney models [102,103],

Table 1
Commonly used biomaterials in 3D bioprinting for urological diseases.

	Bioinks	Gelation	Printing Method	Advantages	Disadvantages	Applications
Natural Biomaterials	Collagen	Thermal crosslinking	Extrusion-based	High biocompatibility and cellular adhesion	Low mechanical properties and slow gelation rate	Renal cancer model [112], cartilage regeneration [113–115], meniscus regeneration [116,117]
		Photo crosslinking(Collagen-methacryloyl)	Extrusion-based/ Light-assisted	Relatively higher mechanical properties	Slow gelation rate	Meniscus regeneration [63], muscle regeneration [118]
	Gelatin	Thermal crosslinking	Extrusion-based	High cellular viability	Low printability and slow gelation rate	Bone Regeneration [119]
		Photo crosslinking (GelMA)	Extrusion-based/ Light-assisted	High printability and cellular viability	Low mechanical properties	Bladder cancer model [105], urethral replacement [104], nerve regeneration [40]
	SFMA	Photo crosslinking	Extrusion-based/ Light-assisted	High cellular viability	Low printability	Cartilage regeneration [107,108]
	CSMA	Photo crosslinking	Extrusion-based/ Light-assisted	High biocompatibility and cellular adhesion	Low printability	Cartilage regeneration [109]
	HAMA	Photo crosslinking	Extrusion-based/ Light-assisted	High cellular viability	Low printability	Cartilage regeneration [110]
	Alginate	Chemical crosslinking	Extrusion-based	High gelation rate	Low printability and weak cellular adhesion	Kidney regeneration [120], hair follicle regeneration [121]
	Agarose	Thermal crosslinking	Extrusion-based	Relatively high mechanical properties stability	Weak cellular adhesion and poor biodegradability	Wound-dressing [122], vascularization [123], neural tissue engineering [124]
	Matrigel	Thermal crosslinking	Extrusion-based	High biocompatibility and cellular adhesion	Low mechanical properties and slow gelation rate	Cancer models [125], liver microfluidic chip [126]
	dECM	Thermal/chemical crosslinking	Extrusion-based	High biocompatibility and cellular adhesion	Low printability	Kidney regeneration [102]
Synthetic Biomaterials	PCL	Solidification	Extrusion-based/ electrowritten	High printability and mechanical properties	Low biodegradation rate	Urethral replacement [127], PCa models [128,129]
	Polylactic acid (PLA)	Solidification	Extrusion-based	Good mechanical strength and processability	Brittleness, poor thermal stability, low crystallinity	Nerve [130], cardiovascular [131]
	Poly (ether ether ketone) (PEEK)	Solidification	Extrusion-based/ light-assisted	High printability and biocompatible	Biological inert	Bone tissue engineering [132]

urethral tubes [104], and bladder cancer models [105,106]. Similar methylation modifications were applied to other natural biomaterials to enhance their printability. Silk fibroin (SF) can be extracted from silkworms and has become a popular biomaterial due to its exceptional mechanical properties. After functionalization with methacrylic anhydride (MA) groups, SF-methacryloyl scaffolds (SFMA) were able to promote the proliferation and differentiation of chondrocytes and further used as DLP bioinks to create scaffolds for cartilage regeneration [107,108]. Chondroitin sulfate [109] (CS) and hyaluronic acid [110] (HA) were also functionalized with MA and investigated for cartilage regeneration. Researchers have demonstrated that the inclusion of hyaluronic acid methacrylate and chondroitin sulfate methacrylate could enhance the chondrogenesis and chondrocyte metabolic activity [111] to promote wound healing.

Alginate is an anionic polysaccharide mainly found in brown algae, which is comprised of repeating (1,4)-linked β-D-mannuronic sequences (M-blocks) and α-L-guluronic acid sequences (G-blocks) interspersed with MG sequences. It can easily form hydrogel through the interaction between G-blocks and divalent cations through ionic crosslinking. Due to the weak printability of alginate, a supporting bath filled with crosslinking solution is usually applied during the extrusion-based printing process, which can make the gelation take place upon injection [42]. Another method is to use a dual syringe applicator, where alginate solutions and cation solutions are held in separately syringe and meet at the nozzle for gelation. The Young's modulus for alginate could be adjusted from 10 kPa to 600 kPa under various degree of crosslinking and gelation time [133,134], which made it an ideal bioink for urological tissue engineering. Alginate with relatively high mechanical property has been used to 3D bioprint hollow tubes for urethral replacement [104,120]. The urological cancers have increasing mechanical properties during progression and metastasis, which also provide the opportunity to model the stages with different stiffness of alginate in the future.

Agarose is also a commonly used biomaterial, which has shown superior mechanical properties, higher stability, and better printability compare with other biomaterials in tissue engineering [135,136]. Agrose has been used for 3D bioprinting of kidney model after mixing with collagen and Fmoc-dipeptide [85]. Matrigel is a commercialized natural biomaterial, which is a basement membrane extracted from Engelbreth-Holm-Swarm (EHS) mouse sarcoma and contains numerous ECM and growth factors that could closely mimic the chemical properties of natural ECM in urologic organs [137].

Synthetic polymers, like PCL, PLA, and PEEK, with significantly higher mechanical properties compared with natural polymers are more suitable for urethral replacement. Urethra mainly functions as a channel permitting the passage of urine, which requires relatively less biochemical cues and cell involvement to promote the regeneration compared with other urologic tissue engineering. Therefore, the most important properties for an ideal biomaterial that used for urethral replacement are good biocompatibility, high biodegradability, and high mechanical strength [138], since the mechanical properties of urethra could reach ~2 MPa [139]. PCL is a Food and Drug Administration (FDA)-approved synthetic polymer [140]. Zhang et al. had utilized PCL to develop artificial urethra [127]. PLA is a commonly used biodegradable polymer in clinical applications and could break down into lactic acid (LA) or to carbon dioxide and water after contacting with biological media [141]. PEEK is also a commonly used synthetic biomaterial with good

biocompatibility and has been used for medical applications like replacement of prosthesis and stents [142]. Therefore, PLA and PEEK could also have the potential application for urethral replacement.

3. Bioprinting urological organs and tissues

3.1. Kidney regeneration

The most commonly used therapeutic options for ESRD are dialysis and organ transplantation. However, these are limited by the availability of matching donor organs and the high risk of organ rejection. The bioprinting of living organ-like constructs with multiple cell types and biomaterials can be one of the potential solutions for ESRD treatment (See Table 2) [143,144]. Lawlor et al. applied extrusion-based scaffold-free 3D printing to replace manual generation for creating *in vitro* kidney organoids using human pluripotent stem cells [46]. 3D bioprinting enabled more accurate manipulation of *in vitro* organoid size, cell number and conformation, where the organoid could precisely contain 100, 200 and 500 thousand cells with 1.79 mm, 2.30 mm, and 3.12 mm in diameter, respectively. The results demonstrated that 3D-bioprinted organoids facilitated the manufacture of uniformly patterned kidney tissue sheets, which exhibited improvements in throughput, quality control, scale, and structure, facilitating both *in vitro* and *in vivo* applications of stem cell-derived human kidney tissue. Ali et al. mixed decellularized kidney ECM with gelatin, HA and glycerol to prepare a photo-crosslinkable bioink for extrusion-based 3D printing [102]. Subsequently, primary kidney cells were harvested and bioprinted in a grid structure with size of 10 × 10 as an *in vitro* kidney model, where cells were highly viable and could mature over time. Most importantly, the bioprinted renal constructs exhibited the structural and functional characteristics of native renal tissue. Graham et al. used inkjet-based bioprinting with agarose-based bioink to pattern human embryonic kidney cells and ovine mesenchymal stem cells with tissue equivalent densities (10 [7] cells/ml) with a high droplet resolution of 1 nL (Fig. 3A) [85]. The printed human embryonic kidney cells were reported to proliferate within the printed structures, which suggested that tissue-like structures can be developed and potentially used for kidney regeneration.

The convoluted proximal tubule (PT) is the most frequently damaged site in renal injury. The main function of PT is to absorb and transport 65–80% of nutrients from the renal filtrate into the blood, including salt, water, glucose, and amino acids. The disorder of PT could cause renal Fanconi syndrome with bicarbonaturia, aminoaciduria, phosphaturia, and uricosuria. Therefore, using 3D bioprinting to create *in vitro* PT models for research applications and nephrotoxicity tests has become an attractive direction in tissue engineering. Lin et al. created vascularized proximal tubule with diameter of 250 μm using extrusion-based 3D printing with gelatin-fibronectin bioink [103]. The co-culture of proximal tubule epithelium and vascular endothelium exhibited active albumin uptake and glucose reabsorption (Fig. 3B). The epithelium–endothelium crosstalk was further studied by exposing PT cells to hyperglycemic conditions while monitoring endothelial cell dysfunction, which suggested that 3D-bioprinted kidney tissue can provide a platform for *in vitro* studies of kidney function, disease modeling, and pharmacology. Microfluidic bioprinting is an extrusion-based printing process that can create more accurate and finer fibers. Addario et al. isolated primary murine tubular (pmTECs), endothelial and fibroblast cells and embedded them in alginate bioink to create core-shell tubes that mimic PT constructs [120]. The core-shell tubes with a diameter of 450 μm were able to last for more than one month and successfully supported the cell viability and metabolic activity (Fig. 3C). Although the 3D-bioprinted kidney modes are still far from clinical organ transplantation, their advanced development in recent years has proved their potential in kidney tissue engineering.

3.2. Urethral replacement

Urethral stricture is a common disorder in males. Approximately 0.6% of males are diagnosed with urethral stricture due to a variety of etiological factors like infection, bladder calculi, and renal failure [18]. The incidence of urethral stricture was estimated to be 200–1200 cases per 100,000 individuals, with the increasing incidence for people age over 55. The estimated annual health-care expenditures for male urethral stricture disease in the USA were 191 million dollars [146]. Urethral stricture constitutes the narrowing of urethra due to ischemic spongiofibrosis after trauma or infection [147]. The accumulation of giant multinucleated cells and myofibroblasts at the inflammation site leads to ECM overexpression and fibrosis at the injury site, which could block urination that in turn causes associated complications such as bladder or urethral stones, hydronephrosis, and renal failure [148]. The treatment of urethral stricture requires substitute urethroplasty with an autologous tissue graft, such as buccal mucosa, genital or extragenital skin [149]. However, patients with complex long strictures or proximal hypospadiases may lack appropriate donor tissue for transplantation and exhibit further complications, like inflammation, infection, and donor site morbidity [150]. Tissue engineering has brought a new direction for urethral replacement by developing artificial urethra *in vitro* with the use of 3D bioprinting technology (See Table 2).

Pi et al. fabricated a multilayered tubular construction with inner diameter of 663 μm and outer diameter of 977 μm in a single step using the 3D printing process based on a multichannel coaxial extrusion system [104]. The bioink was composed of GelMA, alginate and eight-arm PEG acrylate (Fig. 4A). The cannular urothelial tissue constructs were

Table 2
Summary of advances in 3D bioprinting for urological organ and tissues.

Bioprinting Strategies	Bioinks	Tissue Types	Key Research Points	References
Extrusion-based	Scaffold free	Human pluripotent stem cells	Facilitate the formation of uniformly patterned kidney tissue sheets	Lawlor [46]
Extrusion-based	Kidney dECM, gelatin, hyaluronic acid, and glycerol	Primary kidney cells	Exhibit the structural and functional characteristics of the native renal tissue	Ali [102]
Extrusion-based	Agarose mixed with Fmoc-dipeptide and collagen	Human embryonic kidney cells, ovine mesenchymal stem cells	Proliferate within the printed structures and could potentially use for kidney	Graham [85]
Extrusion-based	Gelatin-fibronectin	Proximal tubule epithelium and vascular endothelium	Investigation of epithelium–endothelium crosstalk	Lin [103]
Extrusion-based	Alginate	Primary murine tubular, endothelial, and fibroblast cells	Core-shell tubes supported the cell viability and metabolic activity	Addario [120]
Extrusion-based	GelMA, alginate, and eight-arm PEG acrylate	Bladder urothelial cells and smooth-muscle cells	Printed urethra mimics the histology of the native urethra	Pi [104]
Extrusion-based	PCL/Poly(l-lactide-co-ε-caprolactone) (PLCL) and fibrin	Urothelial cells and smooth-muscle cells	Active proliferation and expression of specific biomarkers	Zhang [127]
Extrusion-based	Poly (lactic-co-glycolic acid) (PLGA)/ PCL/Triethyl citrate (TEC)	Mouse fibroblast cells	Mimic the natural urethral tissue in mechanical properties and cell bioactivity	Xu [145]

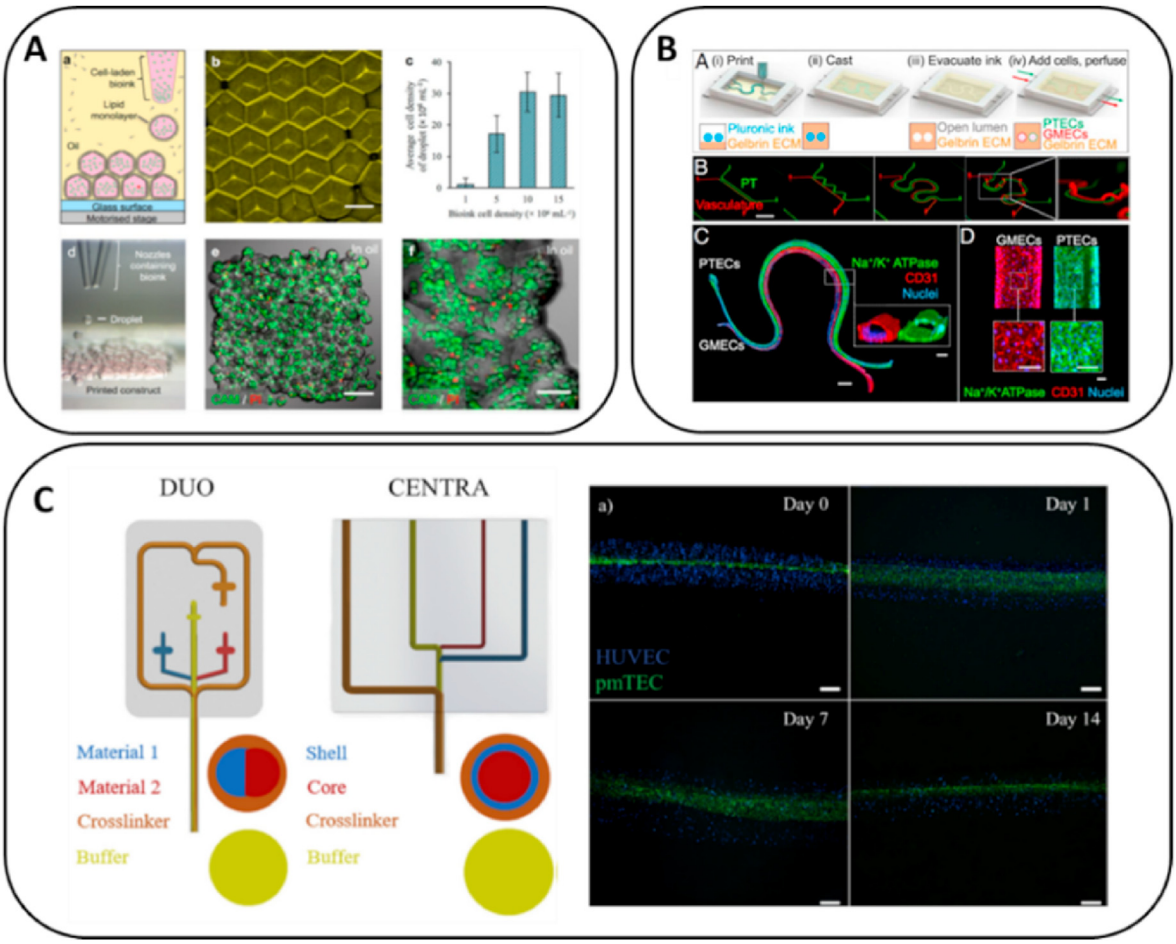

Fig. 3. Bioprinting for kidney regeneration. (a) 3D printing to pattern human embryonic kidney cells and ovine mesenchymal stem cells in high droplet resolution of 1 nL. Adapted with permission [85]. Copyright 2017 Springer Nature (open access); (b) Vascularized proximal tubule using extrusion-based 3D printing. Adapted with permission [103]. Copyright 2017 Frontiers (open access); (c) Micro fluidic bioprinting created core-shell tubes to mimic convoluted proximal tubule. Adapted with permission [120]. Copyright 2020 Elsevier.

bioprinted with bladder urothelial cells for the inner layer and smooth-muscle cells for the outer layer. The printed urethral tube could be actively perfused with fluids. Subsequently, the expression of cell–cell adhesion molecules by urothelial cells and that of α-smooth-muscle actin by smooth-muscle cells were observed, confirming that the printed urethra was able to mimic the histology of native urethra. Zhang et al. utilized extrusion-based 3D bioprinting to develop a cell-laden urethra using different polymer types, PCL/PLCL and fibrin-based hydrogel [127]. The PCL/PLCL scaffold closely mimicked the mechanical characteristics of native urethra (Fig. 4B). The urothelial cells and smooth-muscle cells were printed with fibrin-based hydrogel onto the inner and outer surfaces of PCL/PLCL scaffold, respectively. The multilayer tube has height of 2 cm, inner diameter of 3.2 mm and outer dimeter of 4.7 mm, which closely mimic the human urethra equivalent size. Cells in the hydrogel demonstrated more than 80% viability within 7 days and showed active proliferation and the expression of specific biomarkers, including AE1/AE3 pan-cytokeratin, smooth muscle actin, and myosin. Xu et al. used PLGA/PCL/TEC that had good biodegradability and mechanical properties for the extrusion-based 3D printing of tubular structure with diameter of ~4 cm [145]. This was used to culture mouse fibroblast cells, L929, whose growth characteristics are similar to those of urothelial cells, which proved the good biocompatibility and cell adhesion of the printed urethral tube (Fig. 4C). The results provided the groundwork for further investigations promoting urethral replacement by 3D printing fabricating tubular constructs that mimic the natural urethral tissue in its mechanical properties and cell bioactivity.

4. Bioprinting to mimic the urological TME

4.1. TME

The TME includes cancer cells and the surrounding environment, such as ECM, growth factors, and cancer-associated fibroblasts (CAF). The TME has been demonstrated not only to physically support tumor growth but also to biochemically promote tumor development and metastasis [151]. Therefore, using 3D bioprinting to create an *in vitro* TME for the investigation of cancer cell growth and metastasis mechanism has become an important research direction.

The ECM is a dynamic network formed by proteins, glycoproteins, proteoglycans, and polysaccharides, which not only supports cell growth but also regulates cell proliferation, differentiation, migration, and morphogenesis through cell receptors [152]. One of the major directions in creating *in vitro* TME by bioprinting is to mimic the biomechanical and biochemical properties of ECM using bioinks. For example, type XXIII collagen was found to be upregulated in metastatic PCa cells [153] and a potential biomarker for PCa recurrence [154]. The overexpression of type XXIII collagen also facilitated endothelium adhesion and enhanced cancer cell extravasation during metastasis [155]. Other ECMs, like HA [156], versican [157], laminin [158] and fibronectin [159,160] were also indicated to promote cancer development and metastasis. Therefore, finding methods to mimic ECM biochemical compositions and mechanical properties using bioink is a critical point in bioprinting.

Growth factors and other cell types in the TME could also influence

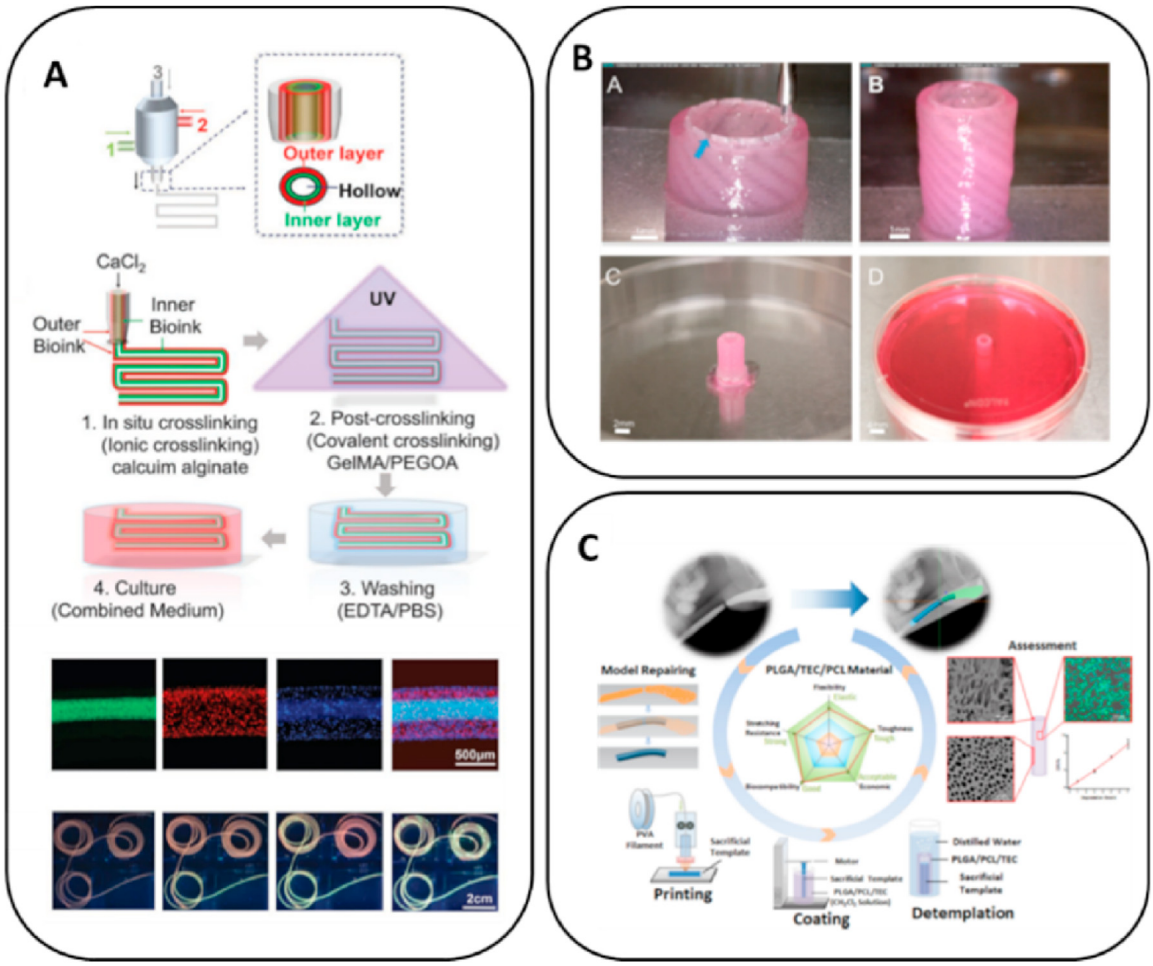

Fig. 4. Bioprinting for urethra replacement. (a) Multilayered tubular construction using multichannel coaxial extrusion system. Adapted with permission [104]. Copyright 2018 Wiley; (b) Cell-laden urethra built with PCL/PLCL and fibrin-based hydrogel. Adapted with permission [127]. Copyright 2017 Elsevier; (c) 3D printed PLGA/PCL/TEC tubular structure. Adapted with permission [145]. Copyright 2020 American Chemical Society.

tumor development. Transforming growth factor-beta (TGF-β) was found to associate with cancer proliferation, motility and apoptosis [161]. The overexpression of vascular endothelial growth factor (VEGF) was able to promote cancer cell invasion [162]. Fibroblast is the principal cell type in connective tissues, which synthesizes ECM and promotes wound healing. However, during cancer development, fibroblasts could transform to CAFs that further facilitate tumor progression, angiogenesis and metastasis through overexpressing ECM and growth factors [163]. The inclusion of multiple cell types and growth factors during the 3D bioprinting process has been widely proved to yield better mimicking of the *in vivo* TME.

Different types of urologic cancers have significant TME heterogeneity including the organ structures, ECM compositions, non-cancer cell types and metastatic sites. Kidney, prostate, and bladder have completely different organ structures. The internal structure of the kidney can be divided into three regions with completely different structures and functions: an outer cortex, a middle-positioned medulla, and the renal pelvis in the deep interior. The prostate also includes three zones: the central zone that surrounds the ejaculatory ducts, the peripheral zone, and the transition zone that surrounds the urethra. Human urinary bladder is a hollow musculo-membranous organ with a triangular shape when contracted and transforms to ovoid as it filled with urine [164].

The proteomics are employed to identify the ECM compositions of urologic cancers. Clear cell renal cell carcinoma (ccRCC) is found that the collagen type VI, fibronectin, and tenascin C are significantly upregulated compared with healthy kidney cortex [165]. CRPC has upregulation of collagen type I, fibronectin, vitronectin, and laminin compared with normal prostate tissues [166]. Bladder cancer has fibrinopeptide A, collagen type I, and uromodulin upregulation [167]. Although urologic cancers have several similar upregulated ECM compositions like collagen and fibronectin, most of the deregulated protein types are different.

Non-cancer cells in the TME, like cancer-associated fibroblasts, immune cells, stromal cells, endothelial cells and epithelial cells, could also promote or inhibit the cancer progression and metastasis [49]. Different urologic organs contain various non-cancer cell types in the TME. Kidney contains at least 16 different highly specialized epithelial cell types, and the number of specialized endothelial cells, immune cells, and interstitial cell types may even be larger [168]. Human prostate also contain three unique epithelial cell types including, basal, luminal, and neuroendocrine [169]. Bladder also contains specific cells like bladder interstitial cells and bladder smooth muscle cell, which are related with bladder regeneration and involved in the complex cellular signaling processes that govern bladder filling and emptying [170,171].

3D bioprinting was also commonly used to simulate the TME of metastatic sites for urologic cancers. The most common metastatic sites for kidney cancer, prostate cancer, and bladder cancer are lung [172], bone [173] and lymph node [174], respectively. The microenvironment in those organs is also completely different. Therefore, it would be critical for 3D bioprinting to recapitulate the differences of the urological TME and provide a better cancer model for drug screening or *in vitro* research platform.

4.2. Prostate cancer

Primary PCa is curable with 85% five-year survival rate, while metastatic PCa causes most of the mortalities. PCa cells preferentially metastasize to the bone microenvironment where they exhibit osteomimic properties and break down the bone structure. Therefore, understanding the mechanism of PCa bone metastasis and preventing it from occurring has become a critical research path. Using the benefits of bioprinting, *in vitro* engineered bone structure can be prepared and used as a platform for PCa metastasis research (See Table 3).

Holzapfel et al. applied a 3D printing extrusion system combined with a rotating structure to prepare a hollow tube using medical-grade PCL (mPCL) with diameter of ~6 mm in order to mimic the morphological and functional humanized organ bone; it could be used as a homing site for PCa cell metastasis [175]. Human mesenchymal progenitor cells were seeded on the bone structure, and recombinant human bone morphogenetic protein-7 (rhBMP-7) growth factor was used to induce the metabolism activity and production of ECM components. Upon further culture, the PCa cells demonstrated preference to the engineered bone constructs, proliferated, and developed macro-metastases [175]. This model could be used to investigate the mechanism of PCa cell behavior after metastasizing to the bone microenvironment (Fig. 5A). Based on this study, Shokoohmanda et al. improved extrusion-based 3D printing technology to prepare a hollow tube with similar diameter as previous study to better mimic the bone structure through coating with a layer of calcium phosphate to enhance cell adhesion (Fig. 5B) [176]. Human osteoblasts and patient-derived PCa patient-derived tumor xenograft (PDXs) were indirectly co-cultured on this platform, which showed that PCa cells would present osteomimicry and protein secretion after bone metastasis [176]. Similar studies were performed by Bock et al., in which osteoprogenitor cells were cultured on an 3D-electrowritten scaffolds to create an engineered bone microenvironment containing viable osteoblastic cells, mineral content, ECM, and osteoblast/osteocyte-derived mRNA and proteins (Fig. 5C) [128]. The direct co-culture of PCa cells and osteoprogenitor cells led to cancer cells displaying functional and molecular features consistent with the profile of clinical bone metastases, such as upregulation of alkaline phosphatase and collagen I and downregulation of sclerostin. This electrowritten model presented a potential application for determining the role of bone microenvironment in PCa metastasis and as a personalized drug screening platform.

3D printing models have also been employed to study the cell-cell interaction between fibroblasts and PCa cells. For instance, primary patient-derived CAFs were cultured on a 15 × 15 mm square electrowritten scaffold made with PCL and deposited extensive ECM. PCa cells co-cultured with CAFs demonstrated significant morphological changes compared with the co-culture of non-malignant prostatic fibroblasts. It was also found that the addition of mast cells to the culture enhanced the morphometric transition through a tryptase-mediated mechanism, which was the first instance to find the linkage between mast cells and PCa progression [129]. 3D-printed scaffolds have also been used as drug delivery vehicles. The commonly used PCa chemotherapeutic, doxorubicin, was loaded onto a scaffold and cultured with patient-derived cells. The metabolic activity and proliferation of PCa cells were significantly reduced, which demonstrated that porous 3D-printed scaffolds could be potentially used as an inexpensive approach to locally deliver chemotherapeutics [177].

4.3. Kidney cancer

ccRCC is the most commonly diagnosed kidney cancer histotype with a 5-year survival rate of 70% [181]. Clinical treatment with immune checkpoint inhibitors in combination with anti-angiogenic therapies has demonstrated positive effects on the clinical outcomes for patients with ccRCC, suggesting that the TME facilitates renal cancer development [182]. The TME of more aggressive renal cancers, like papillary RCC (pRCC) and collecting duct carcinomas, was also analyzed and found to have different marker expression for immune infiltration, vasculature, cell proliferation, and epithelial-to-mesenchymal (EMT) transition [183]. Therefore, the influence of TME in renal cancer should be more seriously considered in clinical treatment and better investigated to promote personalized therapies (See Table 3).

Rosette et al. used magnetic bioprinting with scaffold-free to create a co-culture system containing 6250 to 200,000 cells per organoid, where the renal tumor cells are layered on top of primary fibroblasts, thus mimicking the papillary architecture of human tumors [112]. The co-cultured renal tumor cells recapitulated several features of the disease found in humans, which was not observed in monoculture and 2D culture. Bioprinting was also employed to develop a TNT-like structure that successfully recapitulates the intercellular communication. Collagen-based hydrogel mixed with 786-O renal cancer cells was

Table 3
Summary of advances in 3D bioprinting for urological cancers.

Bioprinting Strategies	Bioinks	Tissue Types	Key Research Points	References
Extrusion-based with rotating structure	PCL	Human mesenchymal progenitor cells and PCa cells	PCa cells demonstrate preference to the engineered bone constructs, proliferate, and developed macro-metastases	Holzapfel [175]
Extrusion-based with rotating structure	PCL/calcium phosphate	Human osteoblasts and PDXs	PCa cells have osteomimicry gene expression and protein secretion after bone metastasis	Shokoohmanda [176]
Electrowritten	PCL	Osteoprogenitor cells and PCa cells	Display functional and molecular features consistent with clinical bone metastases profile	Bock [128]
Electrowritten	PCL	Primary patient derived cancer-associated fibroblast, mast cells, and PCa cells	First time that found the linkage between mast cell and PCa progression	Pereira [129]
Extrusion-based	Polyurethane/polyvinyl alcohol	PCa cells	Locally deliver chemotherapeutics	Ahangar [177]
Magnetic bioprinting	Scaffold free	Renal tumor cells and primary fibroblasts	Recapitulated several features of the disease found in humans	Rosette [112]
Extrusion-based	Collagen-based	Renal cancer cells	Highly controlled and reproducible TME	Herradamanchon [86]
Extrusion-based and microfluidic devices	Ethoxylated bisphenol A diacrylate/tripropyleneglycol diacrylate	Renal cancer cells	Prognostic and therapeutic implications for cancer treatments	Chen [178]
Extrusion-based	GelMA	Bladder cancer cells	Closely mimic the *in vivo* TME	Kim [105]
Piezoelectric inkjet printing	Scaffold free	Bladder cancer cells	Potential method to analyze intratumoral heterogeneity	Yoon [179]
Acoustic droplet printer	Matrigel	Bladder cancer cells and T cells	Provide a platform for personalized tumorimmunotherapy	Gong [180]
Extrusion-based and microfluidic devices	GelMA	Bladder cancer cells and HUVEC	Predict effects of immunotherapeutic agent in bladder cancer	Kim [106]

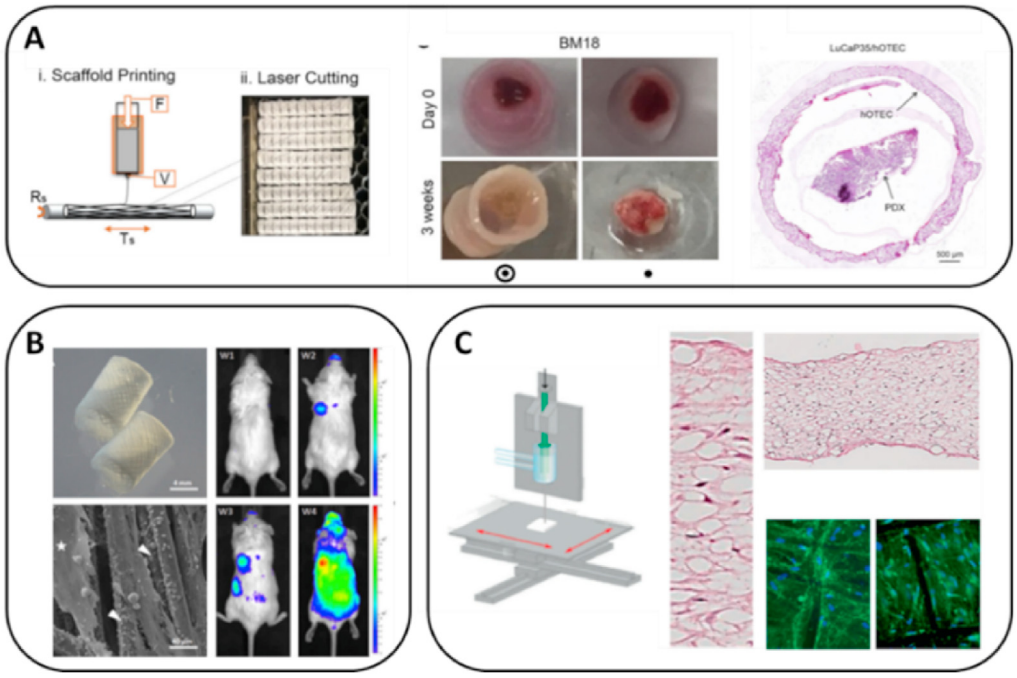

Fig. 5. The application of 3D bioprinting in mimicking PCa TME. (a) Combining 3D printing extrusion system with a rotating structure to prepare a hollow tube that mimics bone structure. Adapted with permission [175]. Copyright 2014 Elsevier; (b) Hollow tube coating with a layer of calcium phosphate to better mimic the chemical properties of human bone and enhance the cell adhesion. Adapted with permission [176]. Copyright 2019 Elsevier; (c) 3D electrowritten scaffolds to prepare an engineered bone microenvironment. Adapted with permission [128]. Copyright 2019 Springer Nature.

bioprinted using extrusion-based printing and conducive to the growth of TNT-like cellular projections inside the hydrogel, showing direct contacts between distant cells (Fig. 6A) [86]. The bioprinted model has diameter of 35 mm and height of 0.15 mm, which provided a highly controlled and reproducible TME to investigate the relevance of TNT-like structures in tumorigenesis and anticancer drug susceptibility. In addition to bioprinting with cells, microfluidic devices for the isolation of CTCs could also be fabricated by extrusion-based 3D printing using hybrid synthetic polymers, including ethoxylated bisphenol A diacrylate and tripropyleneglycol diacrylate. The microfluidic devices have important prognostic and therapeutic implications for cancer treatments (Fig. 6B) [178]. Their capture efficiency could be higher than 90% for the renal cancer cell line 293T, which could be a potential future direction for clinical diagnosis and cancer treatment combined with DNA-based detection. Overall, 3D bioprinting has shown its potential applications in mimicking kidney TME for *in vitro* drug screening, fundamental investigations, and CTCs

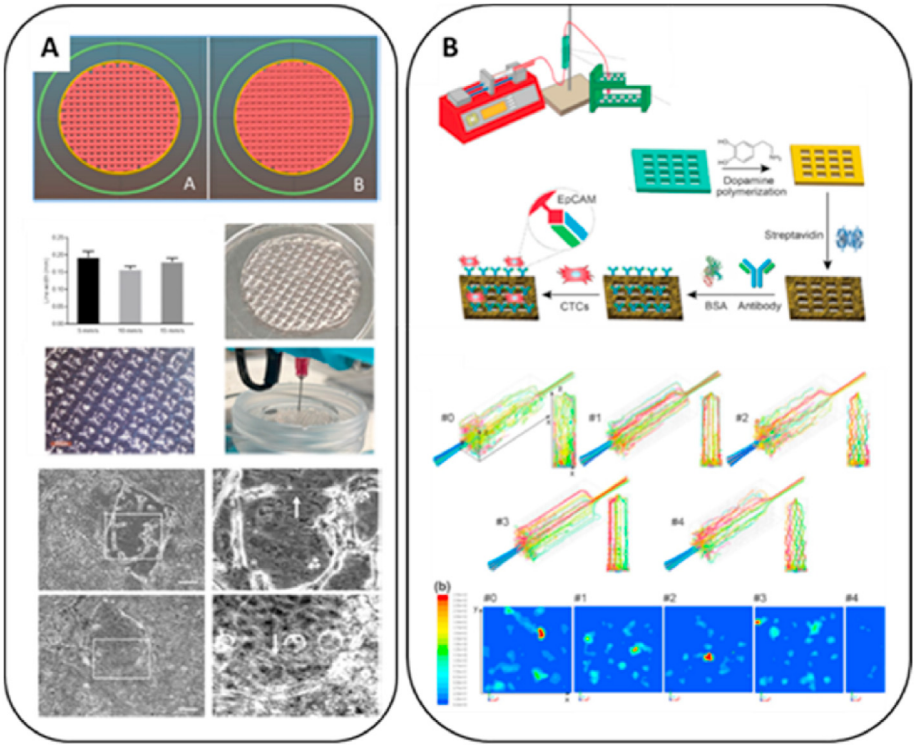

Fig. 6. The application of 3D bioprinting in mimicking kidney TME. (a) Bioprinting develops a tunneling nanotube (TNT)-like structure. Adapted with permission [86]. Copyright 2021 Elsevier; (b) Microfluidic devices for circulating tumor cells (CTCs) isolation. Adapted with permission [178]. Copyright 2020 Elsevier.

isolation, which could be the future direction for kidney cancer treatment.

4.4. Bladder cancer

Bladder cancer is one of the most malignant diseases of the urinary system. It can be classified into three categories based on the progression status: non-muscle invasive bladder cancer, muscle invasive bladder cancer, and metastatic bladder cancer [184]. Recently, immune therapy targeting the PD-1/L1 checkpoint pathway was found to be effective for metastatic bladder cancers, while it was also reported that the bladder TME is able to promote and inhibit the antitumor immune response. Therefore, a deeper understanding of how TME affects cancer cell metastasis is necessary to improve existing bladder cancer treatments (See Table 3).

Using GelMA as a bioink, bladder cancer cells 5637 and T24 were bioprinted to a grid structure with size of 2.5 cm × 2.5 cm × 0.1 mm using extrusion-based bioprinter (Fig. 7A) [105]. The cell proliferation, chemoresistance and EMT marker expression were analyzed to evaluate the occurrence of cancer cell metastasis. Both cell types showed higher cell proliferation rate in the bioprinted constructs compared with 2D and their drug resistance was also upregulated. Under the inducement of TGF-β, bioprinted cells demonstrated the upregulation of N-cadherin and downregulation of E-cadherin, which more closely mimicked the cell behavior in the *in vivo* TME. Piezoelectric inkjet printing is a unique bioprinting method that can be used to investigate tumor heterogeneity. It is able to convert electric signals to physical forces that are in turn used to eject picoliter droplets, which contain an average of 0.70–1.42 cells per droplet [56]. Single primary bladder cancer cells were printed using inkjet bioprinting with scaffold-free in a 384-well size plate. The expansion of single cells in each well reached organoid size ≥300 μm and demonstrated various drug resistance and gene expression characteristics, which suggested that inkjet bioprinting could be a potential method to analyze intratumoral heterogeneity [179]. Gong et al. could also yield bladder cancer organoids using an acoustic inkjet bioprinter, where mouse primary bladder tumor cells were cultured with immune cells in Matrigel with sized of 150–200 nL containing 6000 cells to retain the immune microenvironment similar to primary tissue for more than two weeks (Fig. 7B) [180]. The bioprinted co-culture system more realistically mimicked the TME and could be a novel *in vitro* model system for personalized immunotherapy. Combining 3D bioprinting with microfluidic technology, Kim et al. used extrusion-based bioprinting to create a grid structure with size of 6 mm × 6 mm × 1 mm for bladder cancer cells and HUVEC, which was further combined with a cancer-on-a-chip device (Fig. 7C) to simulate the bladder cancer TME. The effects of TME were evaluated by assessing the immunologic reactions in response to different concentrations of Bacillus Calmette–Guérin, which showed promising results for predicting the effects of immunotherapeutic agents in bladder cancer [106].

5. Discussion

The progress on the application of bioprinting in urological diseases has been remarkable in the past decades. However, many challenges remain for researchers to tackle in order to translate these technologies for clinical applications, which mainly regard technical difficulties of replicating the heterogeneity of urological organs and the selection of materials for recapitulating the complicated ECM components.

5.1. Challenges in the simulation of organ heterogeneity

Various urologic organs have specific microstructures that maintains the organ functions, causing difficulties for *in vitro* simulation using 3D bioprinting. The internal structure of the kidney can be divided into three

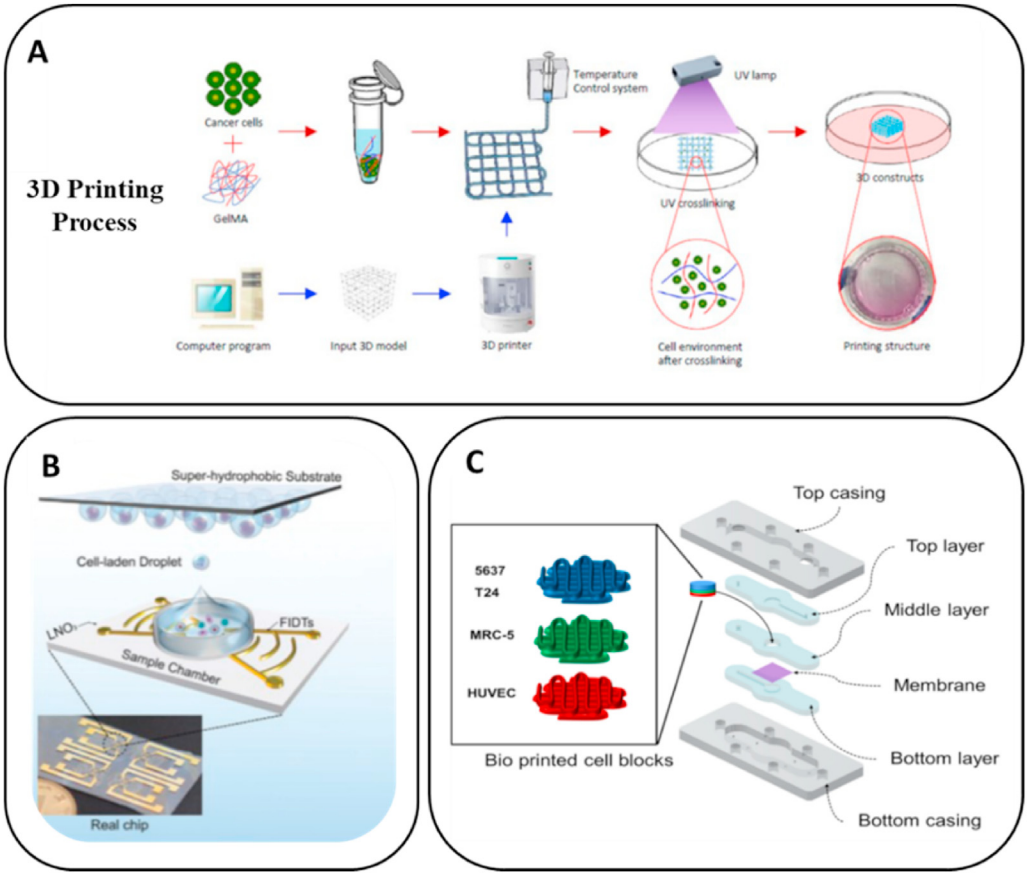

Fig. 7. The application of 3D bioprinting in mimicking bladder cancer TME. (a) Bioprinted grid structure containing bladder cancer cells to evaluate metastasis. Adapted with permission [105]. Copyright 2019 Public Library of Science; (b) Immune cells and bladder cancer cells co-culture system built with acoustic droplet printing. Adapted with permission [180]. Copyright 2021 Wiley; (c) Bladder cancer-on-a-chip developed with bioprinting and microfluidic technology. Adapted with permission [106]. Copyright 2021 MDPI.

regions with completely different structures and functions: an outer cortex, a middle-positioned medulla, and the renal pelvis in the deep interior. The prostate also includes three zones: the central zone that surrounds the ejaculatory ducts, the peripheral zone, and the transition zone that surrounds the urethra. The bladder is a hollow organ that consists of three distinct layers: urothelium, adventitia and muscularis propria. The urothelial layer can be further subdivided into three layers composed by different cell types: umbrella cells, intermediate cells and basal layer cells. Compared with tissue-engineered organs, although *in vitro* cancer models only need to mimic the TME part in the organ, the TME is also complicated due to containing various physical structures (fibrous or interconnected) and micro-vessel distributions. Despite the development of multi-ink/head bioprinters in recent years, the methods toward developing meaningful *in vitro* disease models that mimic tissue heterogeneity with sufficient precision and accuracy are still limited. Extrusion-based bioprinting has been particularly suitable for creating tissue heterogeneity, since the syringe heads are interchangeable and easily positioned on the printing axis. However, the limitation is that *in vivo* tissues have scales that are much lower than what the current extrusion printers can achieve. Although laser-based bioprinting methods, like DLP, two-photon polymerization and light/laser rostering lithography, have the ability to pattern tissues with single-cell resolution, they are lagging behind mostly due to the limited range of viable bioinks and difficulties in manufacturing large-scale constructs. Microfluidic chips have been developed to overcome this challenge. Specifically, hydrogels with different compositions and cell types were connected to a syringe pump and flow to a microdevice in a coordinated procedure under the exposure of light, such that layer-by-layer multimaterial bioprinting of different shapes and structures could be achieved. This strategy may point to a potential method in the future, although still has limitations in the development of Z axis with increasing volume.

Further to the complexity of organ physical structure, the mimicking of cellular types and distributions are also critical in tissue engineering. There are at least 16 different highly specialized epithelial cell types in mammals, and the number of specialized endothelial cells, immune cells, and interstitial cell types may even be larger in the kidney [168]. Human renal glomerular endothelial cells are a specialized microvascular cell type involved in the regulation of glomerular ultrafiltration [185]. Renal tubular epithelial cells are the main regulators of blood pressure, sodium transport and tubulointerstitial fibrosis [186,187]. The concerted interplay between different cell types is critical for normal kidney function. Similar to the difficulties in mimicking organ structures, although the extrusion-based bioprinter can be designed with multiple printing heads containing various cell types, it is still limited by the achievable precision and accuracy to distribute specific cells to certain positions. Light-based printing is also burdened by the difficulties encountered when changing the material/cell bath during the printing process. Inkjet bioprinting could be the most suitable technology for precise cellular distribution. As mentioned in Section 3.2, this technology can be used to generate single cells in a precise pattern with extreme high resolution, since the size of a single droplet can be less than 10 pL.

5.2. Limitations to the development of bioinks

The ECM not only provides structural stability but also mediates cellular responses and is involved in development and organ formation. The re-modification of ECM chemical compositions and mechanical properties have a critical influence on the development of urologic diseases, like renal fibrosis and protein enrichment in PCa. Therefore, the development of 3D-printable biomaterials that could mimic the chemical compositions and physical properties of native ECM is one of the major existing material challenges. Most of the commonly used bioprinting materials, such as GelMA, alginate, and chitosan, have good printability for extrusion-based bioprinting and DLP, whilst they are single-composition, hence fail to recapitulate the matrix composition of a given organ [188]. Therefore, many studies have pointed toward the desirable combination of biomaterials, like gelatin/fibronectin to mimic the proximal tubule [103]. Synthetic biomaterials have also been mixed with biomaterials to enhance the mechanical properties, such as PCL/PLCL/fibrin hydrogel developed for urethral replacement [127]. Although Matrigel contains numerous types of proteins and growth factors, the top three major proteins in Matrigel are constant, including laminin, collagen IV, and entactin/nidogen, which causes the limitation on mimicking the heterogeneity of ECM components for urologic tissue engineering and TME. The application of dECM seems to be one of the most promising directions to mimic the ECM diversity, as it has the closest physical structure, biocompatibility, biomechanics, cell interaction ligands, and growth factors to native tissues [35], and it also retains the ability to induce tissue regeneration [189]. As mentioned previously, a photo-crosslinking hydrogel made with kidney dECM, gelatin, HA, and glycerol has been successfully used for renal regeneration [102]. However, dECM often has poor mechanical properties compared with synthetic polymers, limiting its applications in urological tissue engineering, such as urethral replacement.

Cell-laden bioprinting is a more advanced technology in tissue engineering, since it has the ability to more precisely pattern cells in specific sites and encapsulate them in the ECM, which results in better mimicking the *in vivo* microenvironment. However, the controversy between the bioink mechanical properties and cellular viability during cell-laden bioprinting has limited its application. From the printing perspective, an ideal bioink should possess proper mechanical and rheological properties to generate tissue constructs with adequate mechanical strength, robustness and high shape fidelity [190]. Nonetheless, the better printability of bioink commonly leads to lower cellular viability during cell-laden bioprinting, since cells face much stronger external forces, such as compression stress and shear stress, which narrows down the application of cell-laden bioprinting to fabricating hard tissues, like the bone microenvironment for PCa metastasis model.

Another important challenge for the development of bioinks is their interaction with the host immune system. Even kidney transplantation has a high risk of organ rejection, not to mention the use of engineered organs/tissues, even if they are created with natural materials. The immune system is not only a contributor to kidney regeneration but also a protective strategy against materials of unknown sources [191]. The use of immune-compatible materials, like dECM and fibrin, can substantially minimize the risk of an adverse immune response toward the engineered tissue. However, such natural biomaterials often need to be combined with synthetic polymers to enhance the overall mechanical properties for wider application, like PCL/PLCL/fibrin used for urethral replacement [127]. The paradox here is that hybrid materials have a higher potential to cause immune rejection, which is a challenge to be conquered for the more advanced development of 3D bioprinting.

5.3. Future perspectives

In order to achieve a more advanced level of 3D bioprinting application in urological diseases, the mutual development of printing technics, structural design, bioinks, engineered cells, and conjugation of growth factors needs to be addressed (Fig. 8).

Currently, there has been a technological explosion in bioprinting hardware development and the bioprinting market could reach ~4.1 billion US dollars by 2026 [192]. Numerous commercial bioprinters has been developed with a large price range for pharmaceutical companies and research institutes. Due to the affordability and simplicity, most of the commercial bioprinters are extrusion-based, which could use value adds-on to provide more affordable and accessible 3D bioprinters for customization. Relatively cheaper 3D bioprinters commonly has only one or two extruders, small range of temperature control, less robotic arms and relatively low accuracy, which can be used to print simple structure and is more suitable for industrial application. More advanced extrusion-based bioprinter could have more than three extruders with various temperature control for different types of biomaterials, like

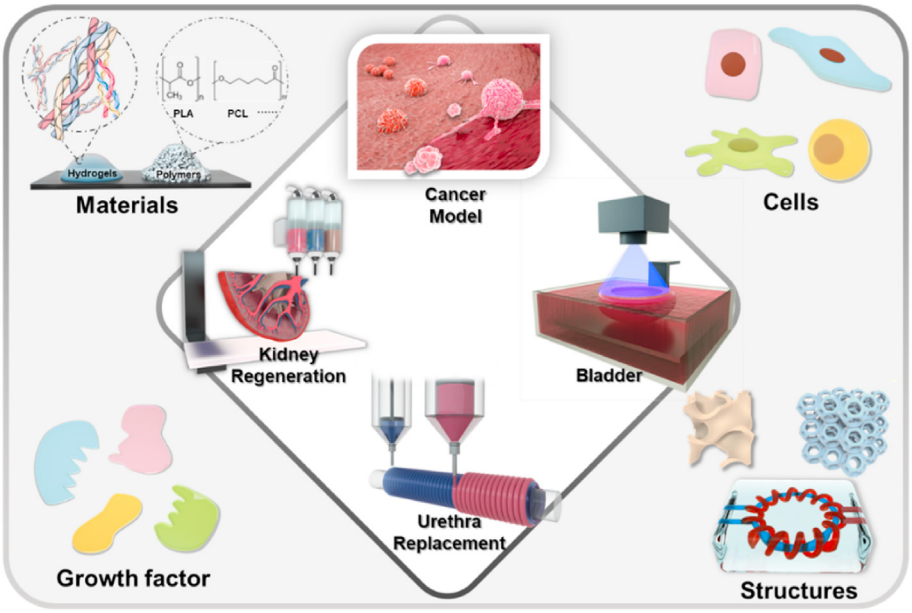

Fig. 8. The development of 3D bioprinting in urological diseases needs the cooperation of printing technics, structure design, biomaterials, engineered cells, and growth factors.

CELLINK BIO X6 bioprinter, which consists of six extruders that allow fast and versatile multi-material bioprinting. Compared with commercial extrusion-based bioprinters, inkjet bioprinters and light-assisted bioprinters on the market are more limited with high cost. RASTRUM 3D inkjet desktop bioprinter by Inventia is able to deposit eight different droplets of cells and matrix components as small as 5 nL [192]. The digital light processing bioprinter developed by Engineering For Life has been used to develop artificial nerve conduits using GelMA [193]. More sophisticated bioprinter could combine more than one printing technologies, like L-series bioprinter developed by MEDPRIN could be customized to contain extrusion-based printhead and melt electro-writing heads for more complicated structure fabrication. A hybrid fabrication platform developed by Yang's research group even combined the extrusion-based and inkjet-based printing together, which is flexible and suitable for a large range of bioinks, including natural biomaterials, synthetic biomaterials, cell aggregates or composites to simulate the complex composition of heterogeneous tissues [194]. Overall, bioprinters with relatively low cost commonly has less functions and low accuracy, which could be more suitable for simple structure fabrication and mass production. Sophisticated bioprinters that contain more than one 3D printing technology could be the future trend for bioprinter development, since each 3D bioprinting technique has its own benefits and limitations, which makes it impossible to create an ideal tissue-engineered urological organ with a single method.

Due to the complicated urologic organ structure, the fabrication of urological organs could be approached with the strategy of automobile or smartphone manufacturing where the components may be prepared using different techniques in various labs and finally assembled together. For example, extrusion-based bioprinting could be used to create the macrostructure of the kidney; light-assisted bioprinting could be applied for the creation of microvessels; and inkjet bioprinting could be employed for precise cell distribution. The development of bioink should consider the results of proteomics for ECM compositions of urologic organs. The short peptide mixture or the dECM application could be the future direction for bioink development. Overall, the development of 3D bioprinting in urological diseases requires stepping up improvements in multidisciplinary fields.

6. Conclusions

Although the clinical application of 3D printing in urological diseases still faces various challenges, evidence has accumulated from numerous studies to prove that this is an achievable goal. Therefore, future work should focus initially on 3D printing technologies and printable biomaterials to truly progress the field forward. There has been a technological explosion in bioprinting hardware development in recent years. The cost of bioprinters has reduced to a few thousand dollars, which significantly reduces the barrier for researchers from different fields to collaborate on investigating 3D printing procedures. Engineers need to work more closely with biologists to enable adapting engineering tools for biological problems, rather than focusing heavily on speed and cost.

Declaration of competing interest

The authors declare the following financial interests/personal relationships which may be considered as potential competing interests: Jun Yin reports financial support was provided by National Key Research and Development Program of China (Grant No. 2018YFA0703000).

References

[1] D.C. Miller, C.S. Saigal, M.S. Litwin, The demographic burden of urologic diseases in America, Urol. Clin. 36 (1) (2009) 11–27.
[2] B. Bikbov, C.A. Purcell, A.S. Levey, M. Smith, A. Abdoli, M. Abebe, Global, regional, and national burden of chronic kidney disease, 1990–2017: a systematic analysis for the Global Burden of Disease Study 2017, Lancet 395 (2020) 709–733.
[3] K. Jansen, C.C.L. Schuurmans, J. Jansen, R. Masereeuw, T. Vermonden, Hydrogel-based cell therapies for kidney regeneration: current trends in biofabrication and in vivo repair, Curr. Pharmaceut. Des. 23 (26) (2017) 3845–3857.
[4] A.J. Peired, B. Mazzinghi, L. De Chiara, F. Guzzi, L. Lasagni, P. Romagnani, E. Lazzeri, Bioengineering strategies for nephrologists: kidney was not built in a day, Expet Opin. Biol. Ther. 20 (5) (2020) 467–480.
[5] N.M. Wragg, L. Burke, S.L. Wilson, A critical review of current progress in 3D kidney biomanufacturing-advances, challenges, and recommendations, Renal Replace. Ther. 5 (1) (2019).
[6] R.L. Siegel, K.D. Miller, H.E. Fuchs, A. Jemal, Cancer statistics, 2021, CA A Cancer J. Clin. 71 (1) (2021) 7–33.
[7] B.I. Rini, S.C. Campbell, B. Escudier, Renal cell carcinoma, Lancet 373 (9669) (2009) 1119–1132.
[8] S. Safiri, A.A. Kolahi, M.A. Mansournia, A. Almasi-Hashiani, A. Ashrafi-Asgarabad, M.J.M. Sullman, D. Bettampadi, M. Qorbani, M. Moradi-Lakeh, M. Ardalan, A. Mokdad, C. Fitzmaurice, The burden of kidney cancer and its attributable risk

factors in 195 countries and territories, 1990-2017, Sci. Rep. 10 (1) (2020), 13862.
[9] S.A. Padala, A. Barsouk, K.C. Thandra, K. Saginala, A. Mohammed, A. Vakiti, P. Rawla, A. Barsouk, Epidemiology of renal cell carcinoma, World J. Oncol. 11 (3) (2020) 79–87.
[10] J. Dobruch, S. Daneshmand, M. Fisch, Y. Lotan, A.P. Noon, M.J. Resnick, S.F. Shariat, A.R. Zlotta, S.A. Boorjian, Gender and bladder cancer: a collaborative review of etiology, biology, and outcomes, Eur. Urol. 69 (2) (2016) 300–310.
[11] M.G. Cumberbatch, M. Rota, J.W. Catto, C. La Vecchia, The role of tobacco smoke in bladder and kidney carcinogenesis: a comparison of exposures and meta-analysis of incidence and mortality risks, Eur. Urol. 70 (3) (2016) 458–466.
[12] J.Y. Teoh, J. Huang, W.Y. Ko, V. Lok, P. Choi, C.F. Ng, S. Sengupta, H. Mostafid, A.M. Kamat, P.C. Black, S. Shariat, M. Babjuk, M.C. Wong, Global trends of bladder cancer incidence and mortality, and their associations with tobacco use and gross domestic product per capita, Eur. Urol. 78 (6) (2020) 893–906.
[13] D.F. Penson, J.M. Chan, Prostate cancer, J. Urol. 177 (6) (2007) 2020–2029.
[14] L. Bubendorf, A. Schopfer, U. Wagner, G. Sauter, H. Moch, N. Willi, T.C. Gasser, M.J. Mihatsch, Metastatic patterns of prostate cancer: an autopsy study of 1,589 patients, Hum. Pathol. 31 (5) (2000) 578–583.
[15] C.S. Grasso, Y.M. Wu, D.R. Robinson, X. Cao, S.M. Dhanasekaran, A.P. Khan, M.J. Quist, X. Jing, R.J. Lonigro, J.C. Brenner, I.A. Asangani, B. Ateeq, S.Y. Chun, J. Siddiqui, L. Sam, M. Anstett, R. Mehra, J.R. Prensner, N. Palanisamy, G.A. Ryslik, F. Vandin, B.J. Raphael, L.P. Kunju, D.R. Rhodes, K.J. Pienta, A.M. Chinnaiyan, S.A. Tomlins, The mutational landscape of lethal castration-resistant prostate cancer, Nature 487 (7406) (2012) 239–243.
[16] M. Kirby, C. Hirst, E.D. Crawford, Characterising the castration-resistant prostate cancer population: a systematic review, Int. J. Clin. Pract. 65 (11) (2011) 1180–1192.
[17] D.J.S. Bono, S. Oudard, M. Ozguroglu, S. Hansen, J.-P. Machiels, I. Kocak, G. Gravis, I. Bodrogi, M.J. Mackenzie, L. Shen, M. Roessner, S. Gupta, A.O. Sartor, Prednisone plus cabazitaxel or mitoxantrone for metastatic castration-resistant prostate cancer progressing after docetaxel treatment, a randomised open-label trial, Lancet 376 (2010) 1147–1154.
[18] L.A. Hampson, J.W. McAninch, B.N. Breyer, Male urethral strictures and their management, Nat. Rev. Urol. 11 (2014) 43–50.
[19] M. Graefen, B. Beyer, T. Schlomm, Outcome of radical prostatectomy: is it the approach or the surgical expertise? Eur. Urol. 66 (3) (2014) 457–458.
[20] C.B. Anderson, D.F. Penson, S. Ni, D.V. Makarov, D.A. Barocas, Centralization of radical prostatectomy in the United States, J. Urol. 189 (2) (2013) 500–506.
[21] A.D. Asimakopoulos, R. Miano, F. Annino, S. Micali, E. Spera, B. Iorio, G. Vespasiani, R. Gaston, Robotic radical nephrectomy for renal cell carcinoma: a systematic review, BMC Urol. 14 (2014) 75.
[22] K. Kondo, J. Klco, E. Nakamura, M. Lechpammer, J. William G. Kaelin, Inhibition of HIF is necessary for tumor suppression by the von Hippel-Lindau protein, Cancer Cell 1 (2002) 237–246.
[23] S.P. Psutka, D.A. Barocas, J.W.F. Catto, J.L. Gore, C.T. Lee, T.M. Morgan, V.A. Master, A. Necchi, M. Roupret, S.A. Boorjian, Staging the host: personalizing risk assessment for radical cystectomy patients, Eur. Urol. Oncol. 1 (4) (2018) 292–304.
[24] R. Langer, J.P. Vacanti, Tissue engineering, Science 260 (5110) (1993) 920.
[25] D.E. Ingber, V.C. Mow, D. Butler, L. Niklason, J. Huard, J. Mao, I. Yannas, D. Kaplan, G. Vunjak-Novakovic, Tissue engineering and developmental biology: going biomimetic, Tissue Eng. 12 (12) (2006) 3265–3283.
[26] Y.L. Yu, Y.K. Shao, Y.Q. Ding, K.Z. Lin, B. Chen, H.Z. Zhang, L.N. Zhao, Z.B. Wang, J.S. Zhang, M.L. Tang, J. Mei, Decellularized kidney scaffold-mediated renal regeneration, Biomaterials 35 (25) (2014) 6822–6828.
[27] Y. Yu, H. Cui, C. Chen, G. Wen, J. Xu, B. Zheng, J. Zhang, C. Wang, Y. Chai, J. Mei, Hypoxia-inducible Factor-1alpha directs renal regeneration induced by decellularized scaffolds, Biomaterials 165 (2018) 48–55.
[28] A. Atala, S.B. Bauer, S. Soker, J.J. Yoo, A.B. Retik, Tissue-engineered autologous bladders for patients needing cystoplasty, Lancet 367 (9518) (2006) 1241–1246.
[29] S.Y. Chung, Bladder tissue-engineering: a new practical solution? Lancet 367 (9518) (2006) 1215–1216.
[30] A. Raya-Rivera, D.R. Esquiliano, J.J. Yoo, E. Lopez-Bayghen, S. Soker, A. Atala, Tissue-engineered autologous urethras for patients who need reconstruction: an observational study, Lancet 377 (9772) (2011) 1175–1182.
[31] X. Lv, Z. Li, S. Chen, M. Xie, J. Huang, X. Peng, R. Yang, H. Wang, Y. Xu, C. Feng, Structural and functional evaluation of oxygenating keratin/silk fibroin scaffold and initial assessment of their potential for urethral tissue engineering, Biomaterials 84 (2016) 99–110.
[32] P.J. Emans, E.J. Jansen, D. van Iersel, T.J. Welting, T.B. Woodfield, S.K. Bulstra, J. Riesle, L.W. van Rhijn, R. Kuijer, Tissue-engineered constructs: the effect of scaffold architecture in osteochondral repair, J. Tissue Eng. Regenerat. Med. 7 (9) (2013) 751–756.
[33] K. Ye, X. Wang, L. Cao, S. Li, Z. Li, L. Yu, J. Ding, Matrix stiffness and nanoscale spatial organization of cell-adhesive ligands direct stem cell fate, Nano Lett. 15 (7) (2015) 4720–4729.
[34] L. Liu, T. Zhang, C. Li, G. Jiang, F. Wang, L. Wang, Regulating surface roughness of electrospun poly(ε-caprolactone)/β-tricalcium phosphate fibers for enhancing bone tissue regeneration, Eur. Polym. J. 143 (2021).
[35] S.V. Murphy, A. Atala, 3D bioprinting of tissues and organs, Nat. Biotechnol. 32 (8) (2014) 773–785.
[36] S. Lu, J. Zhang, S. Lin, D. Zheng, Y. Shen, J. Qin, Y. Li, S. Wang, Recent advances in the development of in vitro liver models for hepatotoxicity testing, Bio-Design Manuf. 4 (4) (2021) 717–734.
[37] F.M. Wood, Skin regeneration: the complexities of translation into clinical practise, Int. J. Biochem. Cell Biol. 56 (2014) 133–140.
[38] F. Hesselmann, J.M. Focke, P.C. Schlanstein, N.B. Steuer, A. Kaesler, S.D. Reinartz, T. Schmitz-Rode, U. Steinseifer, S.V. Jansen, J. Arens, Introducing 3D-potting a novel production process for artifcial membrane lungs with superior blood fow design, Bio-Design Manuf. 5 (2022) 141–152.
[39] L. Ma, Y. Li, Y. Wu, M. Yu, A. Aazmi, L. Gao, Q. Xue, Y. Luo, H. Zhou, B. Zhang, H. Yang, 3D bioprinted hyaluronic acid-based cell-laden scaffold for brain microenvironment simulation, Bio-Design Manuf. 3 (3) (2020) 164–174.
[40] J. Liu, B. Zhang, L. Li, J. Yin, J. Fu, Additive-lathe 3D bioprinting of bilayered nerve conduits incorporated with supportive cells, Bioact. Mater. 6 (1) (2021) 219–229.
[41] X. Li, Y. Yuan, L. Liu, Y.-S. Leung, Y. Chen, Y. Guo, Y. Chai, Y. Chen, 3D printing of hydroxyapatite/tricalcium phosphate scaffold with hierarchical porous structure for bone regeneration, Bio-Design Manuf. 3 (1) (2019) 15–29.
[42] Z. Wang, S.J. Florczyk, Freeze-FRESH: a 3D printing technique to produce biomaterial scaffolds with hierarchical porosity, Materials 13 (2) (2020).
[43] E. Lepowsky, M. Muradoglu, S. Tasoglu, Towards preserving post-printing cell viability and improving the resolution: past, present, and future of 3D bioprinting theory, Bioprinting 11 (2018).
[44] F. You, B.F. Eames, X. Chen, Application of extrusion-based hydrogel bioprinting for cartilage tissue engineering, Int. J. Mol. Sci. 18 (7) (2017).
[45] X. Liu, M. Hao, Z. Chen, T. Zhang, J. Huang, J. Dai, Z. Zhang, 3D bioprinted neural tissue constructs for spinal cord injury repair, Biomaterials 272 (2021), 120771.
[46] K.T. Lawlor, J.M. Vanslambrouck, J.W. Higgins, A. Chambon, K. Bishard, D. Arndt, P.X. Er, S.B. Wilson, S.E. Howden, K.S. Tan, F. Li, L.J. Hale, B. Shepherd, S. Pentoney, S.C. Presnell, A.E. Chen, M.H. Little, Cellular extrusion bioprinting improves kidney organoid reproducibility and conformation, Nat. Mater. 20 (2) (2021) 260–271.
[47] Y. Wu, B. Ayan, K.K. Moncal, Y. Kang, A. Dhawan, S.V. Koduru, D.J. Ravnic, F. Kamal, I.T. Ozbolat, Hybrid bioprinting of zonally stratified human articular cartilage using scaffold-free tissue strands as building blocks, Adv. Healthcare Mater. 9 (22) (2020), e2001657.
[48] B. Kessel, M. Lee, A. Bonato, Y. Tinguely, E. Tosoratti, M. Zenobi-Wong, 3D bioprinting of macroporous materials based on entangled hydrogel microstrands, Adv. Sci. (Weinh) 7 (18) (2020), 2001419.
[49] H. Qu, Z. Han, Z. Chen, L. Tang, C. Gao, K. Liu, H. Pan, H. Fu, C. Ruan, Fractal design boosts extrusion-based 3D printing of bone-mimicking radial-gradient scaffolds, Research (Wash D C) 2021 (2021), 9892689.
[50] L. Ma, Y. Wu, Y. Li, A. Aazmi, H. Zhou, B. Zhang, H. Yang, Current advances on 3D-bioprinted liver tissue models, Adv. Healthcare Mater. 9 (24) (2020), e2001517.
[51] F.R.S. Lord Rayleigh, On the instability of jets, Proc. Lond. Math. Soc. S1–10 (1878) 4–13.
[52] L.R. F.R.S, Some applications of photography, Nature 44 (1891) 249–254.
[53] X. Cui, T. Boland, D.D. D'Lima, M.K. Lotz, Thermal inkjet printing in tissue engineering and regenerative medicine, Recent Pat. Drug Deliv. Formulation 6 (2) (2012) 149–155.
[54] X. Cui, K. Breitenkamp, M.G. Finn, M. Lotz, D.D. D'Lima, Direct human cartilage repair using three-dimensional bioprinting technology, Tissue Eng. 18 (11–12) (2012) 1304–1312.
[55] B.J. de Gans, P.C. Duineveld, U.S. Schubert, Inkjet printing of polymers: state of the art and future developments, Adv. Mater. 16 (3) (2004) 203–213.
[56] H. Wijshoff, The dynamics of the piezo inkjet printhead operation, Phys. Rep. 491 (2010) 77–177.
[57] X. Li, B. Liu, B. Pei, J. Chen, D. Zhou, J. Peng, X. Zhang, W. Jia, T. Xu, Inkjet bioprinting of biomaterials, Chem. Rev. 120 (19) (2020) 10793–10833.
[58] K. Christensen, C. Xu, W. Chai, Z. Zhang, J. Fu, Y. Huang, Freeform inkjet printing of cellular structures with bifurcations, Biotechnol. Bioeng. 112 (5) (2015) 1047–1055.
[59] S. Hewes, A.D. Wong, P.C. Searson, Bioprinting microvessels using an inkjet printer, Bioprinting 7 (2017) 14–18.
[60] R. Liang, Y. Gu, Y. Wu, V. Bunpetch, S. Zhang, Lithography-based 3D bioprinting and bioinks for bone repair and regeneration, ACS Biomater. Sci. Eng. 7 (3) (2021) 806–816.
[61] A. Thomas, I. Orellano, T. Lam, B. Noichl, M.A. Geiger, A.K. Amler, A.E. Kreuder, C. Palmer, G. Duda, R. Lauster, L. Kloke, Vascular bioprinting with enzymatically degradable bioinks via multi-material projection-based stereolithography, Acta Biomater. 117 (2020) 121–132.
[62] Z. Wang, R. Abdulla, B. Parker, R. Samanipour, S. Ghosh, K. Kim, A simple and high-resolution stereolithography-based 3D bioprinting system using visible light crosslinkable bioinks, Biofabrication 7 (4) (2015), 045009.
[63] W. Li, M. Wang, L.S. Mille, J.A. Robledo Lara, V. Huerta, T. Uribe Velazquez, F. Cheng, H. Li, J. Gong, T. Ching, C.A. Murphy, A. Lesha, S. Hassan, T.B.F. Woodfield, K.S. Lim, Y.S. Zhang, A smartphone-enabled portable digital light processing 3D printer, Adv. Mater. 33 (35) (2021), e2102153.
[64] A. Malekpour, X. Chen, Printability and cell viability in extrusion-based bioprinting from experimental, computational, and machine learning views, J. Funct. Biomater. 13 (2) (2022).
[65] L. Ouyang, R. Yao, S. Mao, X. Chen, J. Na, W. Sun, Three-dimensional bioprinting of embryonic stem cells directs highly uniform embryoid body formation, Biofabrication 7 (4) (2015), 044101.
[66] L. Ning, N. Betancourt, D.J. Schreyer, X. Chen, Characterization of cell damage and proliferative ability during and after bioprinting, ACS Biomater. Sci. Eng. 4 (11) (2018) 3906–3918.

[67] B.A. Aguado, W. Mulyasasmita, J. Su, K.J. Lampe, S.C. Heilshorn, Improving viability of stem cells during syringe needle flow through the design of hydrogel cell carriers, Tissue Eng. 18 (7–8) (2012) 806–815.

[68] H. Gudapati, M. Dey, I. Ozbolat, A comprehensive review on droplet-based bioprinting: past, present and future, Biomaterials 102 (2016) 20–42.

[69] T. Xu, J. Jin, C. Gregory, J.J. Hickman, T. Boland, Inkjet printing of viable mammalian cells, Biomaterials 26 (1) (2005) 93–99.

[70] T. Xu, W. Zhao, J.-M. Zhu, M.Z. Albanna, J.J. Yoo, A. Atala, Complex heterogeneous tissue constructs containing multiple cell types prepared by inkjet printing technology, Biomaterials 34 (1) (2013) 130–139.

[71] D.M. Kingsley, C.L. Roberge, A. Rudkouskaya, D.E. Faulkner, M. Barroso, X. Intes, D.T. Corr, Laser-based 3D bioprinting for spatial and size control of tumor spheroids and embryoid bodies, Acta Biomater. 95 (2019) 357–370.

[72] Y.L. Cheng, F. Chen, Preparation and characterization of photocured poly (epsilon-caprolactone) diacrylate/poly (ethylene glycol) diacrylate/chitosan for photopolymerization-type 3D printing tissue engineering scaffold application, Mater. Sci. Eng. C-Mater. Biol. Appl. 81 (2017) 66–73.

[73] S. Bose, D. Ke, H. Sahasrabudhe, A. Bandyopadhyay, Additive manufacturing of biomaterials, Prog. Mater. Sci. 93 (2018) 45–111.

[74] M. Zhang, R. Lin, X. Wang, J. Xue, C. Deng, C. Feng, H. Zhuang, J. Ma, C. Qin, L. Wan, J. Chang, C. Wu, 3D printing of Haversian bone–mimicking scaffolds, Sci. Adv. 6 (2020) eaaz6725.

[75] F. Xu, H. Ren, M. Zheng, X. Shao, T. Dai, Y. Wu, L. Tian, Y. Liu, B. Liu, J. Gunster, Y. Liu, Y. Liu, Development of biodegradable bioactive glass ceramics by DLP printed containing EPCs/BMSCs for bone tissue engineering of rabbit mandible defects, J. Mech. Behav. Biomed. Mater. 103 (2020), 103532.

[76] X. Ma, C. Yu, P. Wang, W. Xu, X. Wan, C.S.E. Lai, J. Liu, A. Koroleva-Maharajh, S. Chen, Rapid 3D bioprinting of decellularized extracellular matrix with regionally varied mechanical properties and biomimetic microarchitecture, Biomaterials 185 (2018) 310–321.

[77] B. Grigoryan, S.J. Paulsen, D.C.C.D.W. Sazer, C.L.F.A.J. Zaita, P.T. Greenfield, N.J. Calafat, J.P. Gounley, A.H. Ta, F.J.A. Randles, J.E. Rosenkrantz, J.D. Louis-Rosenberg, P.A. Galie, K.R. Stevens, J.S. Miller, Multivascular networks and functional intravascular topologies within biocompatible hydrogels, Science 364 (2019) 458–464.

[78] R. Khoeini, H. Nosrati, A. Akbarzadeh, A. Eftekhari, T. Kavetskyy, R. Khalilov, E. Ahmadian, A. Nasibova, P. Datta, L. Roshangar, D.C. Deluca, S. Davaran, M. Cucchiarini, I.T. Ozbolat, Natural and synthetic bioinks for 3D bioprinting, Adv. NanoBiomed Res. 1 (8) (2021).

[79] C. Benwood, J. Chrenek, R.L. Kirsch, N.Z. Masri, H. Richards, K. Teetzen, S.M. Willerth, Natural biomaterials and their use as bioinks for printing tissues, Bioengineering (Basel) 8 (2) (2021).

[80] N. Ashammakhi, S. Ahadian, C. Xu, H. Montazerian, H. Ko, R. Nasiri, N. Barros, A. Khademhosseini, Bioinks and bioprinting technologies to make heterogeneous and biomimetic tissue constructs, Mater. Today Bio. 1 (2019), 100008.

[81] D.G.K. Rasmussen, L. Boesby, S.H. Nielsen, M. Tepel, S. Birot, M.A. Karsdal, A.L. Kamper, F. Genovese, Collagen turnover profiles in chronic kidney disease, Sci. Rep. 9 (1) (2019), 16062.

[82] Y. Liu, Cellular and molecular mechanisms of renal fibrosis, Nat. Rev. Nephrol. 7 (12) (2011) 684–696.

[83] J.M. Catania, G. Chen, A.R. Parrish, Role of matrix metalloproteinases in renal pathophysiologies, Am. J. Physiol. Ren. Physiol. 292 (3) (2007) F905–F911.

[84] A. Huang, G. Guo, Y. Yu, L. Yao, The roles of collagen in chronic kidney disease and vascular calcification, J. Mol. Med. (Berl) 99 (1) (2021) 75–92.

[85] A.D. Graham, S.N. Olof, M.J. Burke, J.P.K. Armstrong, E.A. Mikhailova, J.G. Nicholson, S.J. Box, F.G. Szele, A.W. Perriman, H. Bayley, High-resolution patterned cellular constructs by droplet-based 3D printing, Sci. Rep. 7 (1) (2017) 7004.

[86] H. Herrada-Manchon, L. Celada, D. Rodriguez-Gonzalez, M. Alejandro Fernandez, E. Aguilar, M.D. Chiara, Three-dimensional bioprinted cancer models: a powerful platform for investigating tunneling nanotube-like cell structures in complex microenvironments, Mater. Sci. Eng. C-Mater. Biol. Appl. 128 (2021), 112357.

[87] M. Ojalill, P. Rappu, E. Siljamaki, P. Taimen, P. Bostrom, J. Heino, The composition of prostate core matrisome in vivo and in vitro unveiled by mass spectrometric analysis, Prostate 78 (8) (2018) 583–594.

[88] H.F.d. Carvalho, S.R. Taboga, P.S.L. Vilamaior, Collagen type VI is a component of the extracellular matrix microfibril network of the prostatic stroma, Tissue Cell 29 (2) (1997) 163–170.

[89] N. Burns-Cox, N.C. Avery, J.C. Gingell, A.J. Bailey, Changes in collagen metabolism in prostate cancer: a host response that may alter progression, J. Urol. 166 (5) (2001) 1698–1701.

[90] J.A. Kiefer, M.C. Farach-Carson, Type I collagen-mediated proliferation of PC3 prostate carcinoma cell line-implications for enhanced growth in the bone microenvironment, Matrix Biol. 20 (2001) 429–437.

[91] K.A. Fitzgerald, J. Guo, E.G. Tierney, C.M. Curtin, M. Malhotra, R. Darcy, F.J. O'Brien, C.M. O'Driscoll, The use of collagen-based scaffolds to simulate prostate cancer bone metastases with potential for evaluating delivery of nanoparticulate gene therapeutics, Biomaterials 66 (2015) 53–66.

[92] L. Bayliss, D.J. Mahoney, P. Monk, Normal bone physiology, remodelling and its hormonal regulation, Surgery (Oxford) 30 (2) (2012) 47–53.

[93] P. Caione, N. Capozza, D. Zavaglia, G. Palombaro, R. Boldrini, In vivo bladder regeneration using small intestinal submucosa: experimental study, Pediatr. Surg. Int. 22 (7) (2006) 593–599.

[94] S.L. Chang, P.S. Howard, H.P. Koo, E.J. Macarak, Role of type III collagen inBladder filling, Neurourol. Urodyn. 17 (1998) 135–145.

[95] D.H. Ewalt, P.S. Howard, B. Blyth, H.M. SnyderIII, J.W. Duckett, R.M. Levin, E.J. Macarak, Is lamina propria matrix responsible for normal bladder compliance? J. Urol. 148 (2) (1992) 544–549.

[96] C.B. Wilson, J. Leopard, D.A. Cheresh, R.M. Nakamura, Extracellular matrix and integrin composition of the normal bladder wall, World J. Urol. 14 (1996) 30–37.

[97] K.J. Aitken, D.J. Bagli, The bladder extracellular matrix. Part II: regenerative applications, Nat. Rev. Urol. 6 (11) (2009) 612–621.

[98] T. Billiet, E. Gevaert, T. De Schryver, M. Cornelissen, P. Dubruel, The 3D printing of gelatin methacrylamide cell-laden tissue-engineered constructs with high cell viability, Biomaterials 35 (1) (2014) 49–62.

[99] K. Xu, X. Liu, X. Li, J. Yin, P. Wei, J. Qian, J. Sun, Effect of electrical and electromechanical stimulation on PC12 cell proliferation and axon outgrowth, Front. Bioeng. Biotechnol. 9 (2021).

[100] G. Jiang, S. Li, K. Yu, B. He, J. Hong, T. Xu, J. Meng, C. Ye, Y. Chen, Z. Shi, G. Feng, W. Chen, S. Yan, Y. He, R. Yan, A 3D-printed PRP-GelMA hydrogel promotes osteochondral regeneration through M2 macrophage polarization in a rabbit model, Acta Biomater. 128 (2021) 150–162.

[101] H. Cui, Y. Yu, X. Li, Z. Sun, J. Ruan, Z. Wu, J. Qian, J. Yin, Direct 3D printing of a tough hydrogel incorporated with carbon nanotubes for bone regeneration, J. Mater. Chem. B 7 (45) (2019) 7207–7217.

[102] M. Ali, A.K. Pr, J.J. Yoo, F. Zahran, A. Atala, S.J. Lee, A photo-crosslinkable kidney ECM-derived bioink accelerates renal tissue formation, Adv. Healthcare Mater. 8 (7) (2019), e1800992.

[103] N.Y.C. Lin, K.A. Homan, S.S. Robinson, D.B. Kolesky, N. Duarte, A. Moisan, J.A. Lewis, Renal reabsorption in 3D vascularized proximal tubule models, Proc. Natl. Acad. Sci. U.S.A. 116 (12) (2019) 5399–5404.

[104] Q. Pi, S. Maharjan, X. Yan, X. Liu, B. Singh, A.M. van Genderen, F. Robledo-Padilla, R. Parra-Saldivar, N. Hu, W. Jia, C. Xu, J. Kang, S. Hassan, H. Cheng, X. Hou, A. Khademhosseini, Y.S. Zhang, Digitally tunable microfluidic bioprinting of multilayered cannular tissues, Adv. Mater. 30 (43) (2018), e1706913.

[105] M.J. Kim, B.H. Chi, J.J. Yoo, Y.M. Ju, Y.M. Whang, I.H. Chang, Structure establishment of three-dimensional (3D) cell culture printing model for bladder cancer, PLoS One 14 (10) (2019), e0223689.

[106] J.H. Kim, S. Lee, S.J. Kang, Y.W. Choi, S.Y. Choi, J.Y. Park, I.H. Chang, Establishment of three-dimensional bioprinted bladder cancer-on-a-chip with a microfluidic system using Bacillus calmette-guerin, Int. J. Mol. Sci. 22 (16) (2021).

[107] G. Cheng, Z. Davoudi, X. Xing, X. Yu, X. Cheng, Z. Li, H. Deng, Q. Wang, Advanced silk fibroin biomaterials for cartilage regeneration, ACS Biomater. Sci. Eng. 4 (8) (2018) 2704–2715.

[108] H. Hong, Y.B. Seo, D.Y. Kim, J.S. Lee, Y.J. Lee, H. Lee, O. Ajiteru, M.T. Sultan, O.J. Lee, S.H. Kim, C.H. Park, Digital light processing 3D printed silk fibroin hydrogel for cartilage tissue engineering, Biomaterials 232 (2020), 119679.

[109] P.A. Levett, D.W. Hutmacher, J. Malda, T.J. Klein, Hyaluronic acid enhances the mechanical properties of tissue-engineered cartilage constructs, PLoS One 9 (12) (2014), e113216.

[110] J.W.S. Hayami, S.D. Waldman, B.G. Amsden, Photo-cross-linked methacrylated polysaccharide solution blends with high chondrocyte viability, minimal swelling, and moduli similar to load bearing soft tissues, Eur. Polym. J. 72 (2015) 687–697.

[111] C.C.L. Schuurmans, M. Mihajlovic, C. Hiemstra, K. Ito, W.E. Hennink, T. Vermonden, Hyaluronic acid and chondroitin sulfate (meth)acrylate-based hydrogels for tissue engineering: synthesis, characteristics and pre-clinical evaluation, Biomaterials 268 (2021), 120602.

[112] K.A. Rosette, S.M. Lander, C. VanOpstall, B.D. Looyenga, Three-dimensional coculture provides an improved in vitro model for papillary renal cell carcinoma, Am. J. Physiol. Ren. Physiol. 321 (1) (2021) 33–46.

[113] S. Liu, C.S. Lau, K. Liang, F. Wen, S.H. Teoh, Marine collagen scaffolds in tissue engineering, Curr. Opin. Biotechnol. 74 (2022) 92–103.

[114] S. Rhee, J.L. Puetzer, B.N. Mason, C.A. Reinhart-King, L.J. Bonassar, 3D bioprinting of spatially heterogeneous collagen constructs for cartilage tissue engineering, ACS Biomater. Sci. Eng. 2 (10) (2016) 1800–1805.

[115] T. Xu, K.W. Binder, M.Z. Albanna, D. Dice, W. Zhao, J.J. Yoo, A. Atala, Hybrid printing of mechanically and biologically improved constructs for cartilage tissue engineering applications, Biofabrication 5 (1) (2012), 015001-015001.

[116] M.B. Pabbruwe, W. Kafienah, J.F. Tarlton, S. Mistry, D.J. Fox, A.P. Hollander, Repair of meniscal cartilage white zone tears using a stem cell/collagen-scaffold implant, Biomaterials 31 (9) (2010) 2583–2591.

[117] J. Heo, R.H. Koh, W. Shim, H.D. Kim, H.G. Yim, N.S. Hwang, Riboflavin-induced photo-crosslinking of collagen hydrogel and its application in meniscus tissue engineering, Drug Deliv. Translation. Res. 6 (2) (2016) 148–158.

[118] W.T. Brinkman, K. Nagapudi, B.S. Thomas, E.L. Chaikof, Photo-Cross-linking of type I collagen gels in the presence of smooth muscle cells-mechanical properties, cell viability, and function, Biomacromolecules 4 (2003) 890–895.

[119] A. Kara, T. Distler, C. Polley, D. Schneidereit, H. Seitz, O. Friedrich, F. Tihminlioglu, A.R. Boccaccini, 3D printed gelatin/decellularized bone composite scaffolds for bone tissue engineering: fabrication, characterization and cytocompatibility study, Mater. Today Bio. 15 (2022), 100309.

[120] G. Addario, S. Djudjaj, S. Fare, P. Boor, L. Moroni, C. Mota, Microfluidic bioprinting towards a renal in vitro model, Bioprinting 20 (2020), e00108.

[121] D. Kang, Z. Liu, C. Qian, J. Huang, Y. Zhou, X. Mao, Q. Qu, B. Liu, J. Wang, Z. Hu, Y. Miao, 3D bioprinting of a gelatin-alginate hydrogel for tissue-engineered hair follicle regeneration, Acta Biomater. (2022).

[122] S. Latiyan, T.S.S. Kumar, M. Doble, Fabrication and evaluation of multifunctional agarose based electrospun scaffolds for cutaneous wound repairs, J. Tissue Eng. Regenerat. Med. 16 (2022) 653–664.

[123] K. Bloch, A. Vanichkin, L.G. Damshkaln, V.I. Lozinsky, P. Vardi, Vascularization of wide pore agarose-gelatin cryogel scaffolds implanted subcutaneously in diabetic and non-diabetic mice, Acta Biomater. 6 (3) (2010) 1200–1205.
[124] D.Y. Lewitus, J. Landers, J. Branch, K.L. Smith, G. Callegari, J. Kohn, A.V. Neimark, Biohybrid carbon nanotube/agarose fibers for neural tissue engineering, Adv. Funct. Mater. 21 (14) (2011) 2624–2632.
[125] G. Benton, I. Arnaoutova, J. George, H.K. Kleinman, J. Koblinski, Matrigel: from discovery and ECM mimicry to assays and models for cancer research, Adv. Drug Deliv. Rev. 79–80 (2014) 3–18.
[126] J.E. Snyder, Q. Hamid, C. Wang, R. Chang, K. Emami, H. Wu, W. Sun, Bioprinting cell-laden matrigel for radioprotection study of liver by pro-drug conversion in a dual-tissue microfluidic chip, Biofabrication 3 (3) (2011), 034112.
[127] K. Zhang, Q. Fu, J. Yoo, X. Chen, P. Chandra, X. Mo, L. Song, A. Atala, W. Zhao, 3D bioprinting of urethra with PCL/PLCL blend and dual autologous cells in fibrin hydrogel: an in vitro evaluation of biomimetic mechanical property and cell growth environment, Acta Biomater. 50 (2017) 154–164.
[128] N. Bock, A. Shokoohmand, T. Kryza, J. Rohl, J. Meijer, P.A. Tran, C.C. Nelson, J.A. Clements, D.W. Hutmacher, Engineering osteoblastic metastases to delineate the adaptive response of androgen-deprived prostate cancer in the bone metastatic microenvironment, Bone Research 7 (2019) 13.
[129] B.A. Pereira, N.L. Lister, K. Hashimoto, L. Teng, M. Flandes-Iparraguirre, A. Eder, A. Sanchez-Herrero, B. Niranjan, A. Melbourne Urological Research, Tissue engineered human prostate microtissues reveal key role of mast cell-derived tryptase in potentiating cancer-associated fibroblast (CAF)-induced morphometric transition in vitro, Biomaterials 197 (2019) 72–85.
[130] H. Matsumine, R. Sasaki, M. Yamato, T. Okano, H. Sakurai, A polylactic acid non-woven nerve conduit for facial nerve regeneration in rats, J. Tissue Eng. Regenerat. Med. 8 (6) (2014) 454–462.
[131] W. Hadasha, D. Bezuidenhout, Poly(lactic acid) as biomaterial for cardiovascular devices and tissue engineering applications, Indus. Appl. Poly(lactic Acid) (2017) 51–77.
[132] J. Zheng, H. Zhao, E. Dong, J. Kang, C. Liu, C. Sun, D. Li, L. Wang, Additively-manufactured PEEK/HA porous scaffolds with highly-controllable mechanical properties and excellent biocompatibility, Mater. Sci. Eng. C-Mater. Biol. Appl. 128 (2021), 112333.
[133] B. Chang, N. Ahuja, C. Ma, X. Liu, Injectable scaffolds: preparation and application in dental and craniofacial regeneration, Mater. Sci. Eng. R Rep. 111 (2017) 1–26.
[134] G. Kaklamani, D. Cheneler, L.M. Grover, M.J. Adams, J. Bowen, Mechanical properties of alginate hydrogels manufactured using external gelation, J. Mech. Behav. Biomed. Mater. 36 (2014) 135–142.
[135] H.M. Butler, E. Naseri, D.S. MacDonald, R.A. Tasker, A. Ahmadi, Investigation of rheology, printability, and biocompatibility of N,O-carboxymethyl chitosan and agarose bioinks for 3D bioprinting of neuron cells, Materialia 18 (2021).
[136] G.R. Lopez-Marcial, A.Y. Zeng, C. Osuna, J. Dennis, J.M. Garcia, G.D. O'Connell, Agarose-based hydrogels as suitable bioprinting materials for tissue engineering, ACS Biomater. Sci. Eng. 4 (10) (2018) 3610–3616.
[137] H.K. Kleinman, G.R. Martin, Matrigel: basement membrane matrix with biological activity, Semin. Cancer Biol. 15 (5) (2005) 378–386.
[138] A. Mangera, C.R. Chapple, Tissue engineering in urethral reconstruction–an update, Asian J. Androl. 15 (1) (2013) 89–92.
[139] C. Feng, Y.M. Xu, Q. Fu, W.D. Zhu, L. Cui, J. Chen, Evaluation of the biocompatibility and mechanical properties of naturally derived and synthetic scaffolds for urethral reconstruction, J. Biomed. Mater. Res., Part A 94 (1) (2010) 317–325.
[140] A. Zimmerling, Z. Yazdanpanah, D.M.L. Cooper, J.D. Johnston, X. Chen, 3D printing PCL/nHA bone scaffolds: exploring the influence of material synthesis techniques, Biomater. Res. 25 (1) (2021) 3.
[141] D. da Silva, M. Kaduri, M. Poley, O. Adir, N. Krinsky, J. Shainsky-Roitman, A. Schroeder, Biocompatibility, biodegradation and excretion of polylactic acid (PLA) in medical implants and theranostic systems, Chem. Eng. J. 340 (2018) 9–14.
[142] A. Haleem, M. Javaid, Polyether ether ketone (PEEK) and its 3D printed implants applications in medical field: an overview, Clin. Epidemiol. Glob. Health 7 (4) (2019) 571–577.
[143] J.E. Arenas-Herrera, I.K. Ko, A. Atala, J.J. Yoo, Decellularization for whole organ bioengineering, Biomed. Mater. 8 (1) (2013), 014106.
[144] M. Nishikawa, Y. Sakai, N. Yanagawa, Design and strategy for manufacturing kidney organoids, Bio-Design Manufact. 3 (1) (2020) 7–14.
[145] Y. Xu, Q. Meng, X. Jin, F. Liu, J. Yu, Biodegradable scaffolds for urethra tissue engineering based on 3D printing, ACS Appl. Bio Mater. 3 (4) (2020) 2007–2016.
[146] R.A. Santucci, G.F. Joyce, M. Wise, Male urethral stricture disease, J. Urol. 177 (5) (2007) 1667–1674.
[147] J.M. Latini, J.W. McAninch, S.B. Brandes, J.Y. Chung, D. Rosenstein, SIU/ICUD Consultation on Urethral Strictures: epidemiology, etiology, anatomy, and nomenclature of urethral stenoses, strictures, and pelvic fracture urethral disruption injuries, Urology 83 (3 Suppl) (2014) S1–S7.
[148] L.S. Baskin, S.C. Constantinescu, P.S. Howard, J.W. Mcaninch, D.H. Ewalt, J.W. Duckett, H.M. Snyder, E.J. Macarak, Biochemical characterization and quantitation of the collagenous components of urethral stricture tissue, J. Urol. 150 (1993) 642–647.
[149] Y.J. Lee, S.W. Kim, Current management of urethral stricture, Kor. J. Urol. 54 (9) (2013) 561–569.
[150] D.N. Wood, S.E. Allen, D.E. Andrich, T.J. Greenwell, A.R. Mundy, The morbidity of buccal mucosal graft harvest for urethroplasty and the effect of nonclosure of the graft harvest site on postoperative pain, J. Urol. 172 (2) (2004) 580–583.
[151] F. Spill, D.S. Reynolds, R.D. Kamm, M.H. Zaman, Impact of the physical microenvironment on tumor progression and metastasis, Curr. Opin. Biotechnol. 40 (2016) 41–48.
[152] C. Frantz, K.M. Stewart, V.M. Weaver, The extracellular matrix at a glance, J. Cell Sci. 123 (Pt 24) (2010) 4195–4200.
[153] J. Banyard, L. Bao, B.R. Zetter, Type XXIII collagen, a new transmembrane collagen identified in metastatic tumor cells, J. Biol. Chem. 278 (23) (2003) 20989–20994.
[154] J. Banyard, L. Bao, M.D. Hofer, D. Zurakowski, K.A. Spivey, A.S. Feldman, L.M. Hutchinson, R. Kuefer, M.A. Rubin, B.R. Zetter, Collagen XXIII expression is associated with prostate cancer recurrence and distant metastases, Clin. Cancer Res. 13 (9) (2007) 2634–2642.
[155] K.A. Spivey, I. Chung, J. Banyard, I. Adini, H.A. Feldman, B.R. Zetter, A role for collagen XXIII in cancer cell adhesion, anchorage-independence and metastasis, Oncogene 31 (18) (2012) 2362–2372.
[156] A. Afify, P. Purnell, L. Nguyen, Role of CD44s and CD44v6 on human breast cancer cell adhesion, migration, and invasion, Exp. Mol. Pathol. 86 (2) (2009) 95–100.
[157] A.D. Theocharis, Versican in health and disease, Connect. Tissue Res. 49 (3) (2008) 230–234.
[158] M.P. Marinkovich, Tumour microenvironment: laminin 332 in squamous-cell carcinoma, Nat. Rev. Cancer 7 (5) (2007) 370–380.
[159] S. Astrof, R.O. Hynes, Fibronectins in vascular morphogenesis, Angiogenesis 12 (2009).
[160] A. Hielscher, K. Ellis, C. Qiu, J. Porterfield, S. Gerecht, Fibronectin deposition participates in extracellular matrix assembly and vascular morphogenesis, PLoS One 11 (1) (2016), e0147600.
[161] Y.N. Niu, S.J. Xia, Stroma-epithelium crosstalk in prostate cancer, Asian J. Androl. 11 (1) (2009) 28–35.
[162] S. Zhang, H.E. Zhau, A.O. Osunkoya, S. Iqbal, X. Yang, S. Fan, Z. Chen, R. Wang, F.F. Marshall, L.W. Chung, D. Wu, Vascular endothelial growth factor regulates myeloid cell leukemia-1 expression through neuropilin-1-dependent activation of c-MET signaling in human prostate cancer cells, Mol. Cancer 9 (2010).
[163] C.E. Weber, P.C. Kuo, The tumor microenvironment, Surg. Oncol. 21 (3) (2012) 172–177.
[164] S. Sharma, B. Basu, Biomaterials assisted reconstructive urology: the pursuit of an implantable bioengineered neo-urinary bladder, Biomaterials 281 (2022), 121331.
[165] K.H. Bond, T. Chiba, K.P.H. Wynne, C.P.H. Vary, S. Sims-Lucas, J.M. Coburn, L. Oxburgh, The extracellular matrix environment of clear cell renal cell carcinoma determines cancer associated fibroblast growth, Cancers (Basel) 13 (23) (2021).
[166] M.J. Mosquera, S. Kim, R. Bareja, Z. Fang, S. Cai, H. Pan, M. Asad, M.L. Martin, M. Sigouros, F.M. Rowdo, S. Ackermann, J. Capuano, J. Bernheim, C. Cheung, A. Doane, N. Brady, R. Singh, D.S. Rickman, V. Prabhu, J.E. Allen, L. Puca, A.F. Coskun, M.A. Rubin, H. Beltran, J.M. Mosquera, O. Elemento, A. Singh, Extracellular matrix in synthetic hydrogel-based prostate cancer organoids regulate therapeutic response to EZH2 and DRD2 inhibitors, Adv. Mater. 34 (2) (2022), e2100096.
[167] A. Latosinska, M. Frantzi, A. Vlahou, A.S. Merseburger, H. Mischak, Clinical proteomics for precision medicine: the bladder cancer case, Proteonomics Clin. Appl. 12 (2) (2018).
[168] M.S. Balzer, T. Rohacs, K. Susztak, How many cell types are in the kidney and what do they do? Annu. Rev. Physiol. 84 (2022) 507–531.
[169] G.H. Henry, A. Malewska, D.B. Joseph, V.S. Malladi, J. Lee, J. Torrealba, R.J. Mauck, J.C. Gahan, G.V. Raj, C.G. Roehrborn, G.C. Hon, M.P. MacConmara, J.C. Reese, R.C. Hutchinson, C.M. Vezina, D.W. Strand, A cellular anatomy of the normal adult human prostate and prostatic urethra, Cell Rep. 25 (12) (2018) 3530–3542, e3535.
[170] K.D. McCloskey, Bladder interstitial cells: an updated review of current knowledge, Acta Physiol. (Oxf) 207 (1) (2013) 7–15.
[171] A. Mirzaei, E. Saburi, M. Islami, A. Ardeshirylajimi, M.D. Omrani, M. Taheri, A.S. Moghadam, S. Ghafouri-Fard, Bladder smooth muscle cell differentiation of the human induced pluripotent stem cells on electrospun Poly(lactide-co-glycolide) nanofibrous structure, Gene 694 (2019) 26–32.
[172] S. Dudani, G. de Velasco, J.C. Wells, C.L. Gan, F. Donskov, C. Porta, A. Fraccon, F. Pasini, J.L. Lee, A. Hansen, G.A. Bjarnason, B. Beuselinck, S.K. Pal, T. Yuasa, N. Kroeger, R. Kanesvaran, M.N. Reaume, C. Canil, T.K. Choueiri, D.Y.C. Heng, Evaluation of clear cell, papillary, and chromophobe renal cell carcinoma metastasis sites and association with survival, JAMA Netw. Open 4 (1) (2021), e2021869.
[173] L. Bubendorf, A. Schöpfer, U. Wagner, G. Sauter, H. Moch, N. Willi, T.C. Gasser, M.J. Mihatsch, Metastatic patterns of prostate cancer: an autopsy study of 1,589 patients, Hum. Pathol. 31 (5) (2000) 578–583.
[174] P.P. Dangle, M.C. Gong, R.R. Bahnson, K.S. Pohar, How do commonly performed lymphadenectomy templates influence bladder cancer nodal stage? J. Urol. 183 (2) (2010) 499–504.
[175] B.M. Holzapfel, F. Wagner, D. Loessner, N.P. Holzapfel, L. Thibaudeau, R. Crawford, M.T. Ling, J.A. Clements, P.J. Russell, D.W. Hutmacher, Species-specific homing mechanisms of human prostate cancer metastasis in tissue engineered bone, Biomaterials 35 (13) (2014) 4108–4115.
[176] A. Shokoohmand, J. Ren, J. Baldwin, A. Atack, A. Shafiee, C. Theodoropoulos, M.L. Wille, P.A. Tran, L.J. Bray, D. Smith, N. Chetty, P.M. Pollock, D.W. Hutmacher, J.A. Clements, E.D. Williams, N. Bock, Microenvironment engineering of osteoblastic bone metastases reveals osteomimicry of patient-derived prostate cancer xenografts, Biomaterials 220 (2019), 119402.

[177] P. Ahangar, E. Akoury, A.S. Ramirez Garcia Luna, A. Nour, M.H. Weber, D.H. Rosenzweig, Nanoporous 3D-printed scaffolds for local doxorubicin delivery in bone metastases secondary to prostate cancer, Materials (Basel) 11 (9) (2018).
[178] J. Chen, C.Y. Liu, X. Wang, E. Sweet, N. Liu, X. Gong, L. Lin, 3D printed microfluidic devices for circulating tumor cells (CTCs) isolation, Biosens. Bioelectron. 150 (2020), 111900.
[179] W.H. Yoon, H.R. Lee, S. Kim, E. Kim, J.H. Ku, K. Shin, S. Jung, Use of inkjet-printed single cells to quantify intratumoral heterogeneity, Biofabrication 12 (3) (2020), 035030.
[180] Z. Gong, L. Huang, X. Tang, K. Chen, Z. Wu, L. Zhang, Y. Sun, Y. Xia, H. Chen, Y. Wei, F. Wang, S. Guo, Acoustic droplet printing tumor organoids for modeling bladder tumor immune microenvironment within a week, Adv. Healthcare Mater. (2021), e2101312.
[181] X. Feng, L. Zhang, W. Tu, S. Cang, Frequency, incidence and survival outcomes of clear cell renal cell carcinoma in the United States from 1973 to 2014: a SEER-based analysis, Medicine (Baltim.) 98 (31) (2019), e16684.
[182] B.I. Rini, E.R. Plimack, V. Stus, R. Gafanov, R. Hawkins, D. Nosov, F. Pouliot, B. Alekseev, D. Soulieres, B. Melichar, I. Vynnychenko, A. Kryzhanivska, I. Bondarenko, S.J. Azevedo, D. Borchiellini, C. Szczylik, M. Markus, R.S. McDermott, J. Bedke, S. Tartas, Y.H. Chang, S. Tamada, Q. Shou, R.F. Perini, M. Chen, M.B. Atkins, T. Powles, K.- Investigators, Pembrolizumab plus axitinib versus sunitinib for advanced renal-cell carcinoma, N. Engl. J. Med. 380 (12) (2019) 1116–1127.
[183] N.C. Synnott, M.L. Poeta, M. Costantini, R.M. Pfeiffer, M. Li, Y. Golubeva, S. Lawrence, K. Mutreja, C. Amoreo, M. Dabrowska, G. Simone, E. Pescarmona, P. Lenz, M. Olanich, M. Duggan, M. Abubakar, V.M. Fazio, M. Gallucci, S. Sentinelli, M.T. Landi, Characterizing the tumor microenvironment in rare renal cancer histological types, J. Pathol.: Clin. Res. 8 (2021) 88–98.
[184] K. Hatogai, R.F. Sweis, The tumor microenvironment of bladder cancer, Adv. Exp. Med. Biol. 1296 (2020) 275–290.
[185] P. Dimou, R.D. Wright, K.L. Budge, A. Midgley, S.C. Satchell, M. Peak, M.W. Beresford, The human glomerular endothelial cells are potent pro-inflammatory contributors in an in vitro model of lupus nephritis, Sci. Rep. 9 (1) (2019) 8348.
[186] R. Qi, C. Yang, Renal tubular epithelial cells: the neglected mediator of tubulointerstitial fibrosis after injury, Cell Death Dis. 9 (11) (2018) 1126.
[187] N. Ramkumar, D. Stuart, E. Mironova, V. Bugay, S. Wang, N. Abraham, A. Ichihara, J.D. Stockand, D.E. Kohan, Renal tubular epithelial cell prorenin receptor regulates blood pressure and sodium transport, Am. J. Physiol.-Renal Physiol. 311 (1) (2016) F186–F194.
[188] L.E. Bertassoni, Bioprinting of Complex Multicellular Organs with Advanced Functionality—Recent Progress and Challenges Ahead, Advanced Materials, 2021.
[189] H.W. Kang, S.J. Lee, I.K. Ko, C. Kengla, J.J. Yoo, A. Atala, A 3D bioprinting system to produce human-scale tissue constructs with structural integrity, Nat. Biotechnol. 34 (3) (2016) 312–319.
[190] P.S. Gungor-Ozkerim, I. Inci, Y.S. Zhang, A. Khademhosseini, M.R. Dokmeci, Bioinks for 3D bioprinting: an overview, Biomater. Sci. 6 (5) (2018) 915–946.
[191] H.J. Anders, Immune system modulation of kidney regeneration–mechanisms and implications, Nat. Rev. Nephrol. 10 (6) (2014) 347–358.
[192] H. Ravanbakhsh, V. Karamzadeh, G. Bao, L. Mongeau, D. Juncker, Y.S. Zhang, Emerging technologies in multi-material bioprinting, Adv. Mater. 33 (49) (2021).
[193] W. Ye, H. Li, K. Yu, C. Xie, P. Wang, Y. Zheng, P. Zhang, J. Xiu, Y. Yang, F. Zhang, Y. He, Q. Gao, 3D printing of gelatin methacrylate-based nerve guidance conduits with multiple channels, Mater. Des. 192 (2020).
[194] H. Zhou, P. Liu, Z. Gao, Q. Li, W. Lv, J. Yin, B. Zhang, H. Yang, L. Ma, Simultaneous multimaterial multimethod bioprinting, Bio-Design Manuf. 5 (2022) 433–436.